COPY NO. 20

TECHNICAL REPORT 4307

SUBSONIC AERODYNAMIC STABILIZATION OF LONG, LOW-DRAG BODIES OF REVOLUTION USING BOATTAIL FINS

ROY W. KLINE

JUNE 1972

PICATINNY ARSENAL
DOVER, NEW JERSEY

The findings in this report are not to be construed as an official Department of the Army Position.

DISPOSITION

Destroy this report when no longer needed. Do not return it to the originator.

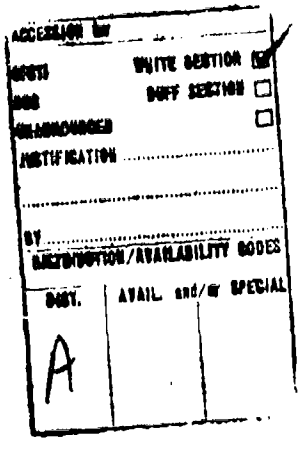

UNCLASSIFIED
Security Classification

DOCUMENT CONTROL DATA - R & D

(Security classification of title, body of abstract and indexing annotation must be entered when the overall report is classified)

1. ORIGINATING ACTIVITY (Corporate author) Picatinny Arsenal, Dover, N. J. 07801	2a. REPORT SECURITY CLASSIFICATION UNCLASSIFIED 2b. GROUP

3. REPORT TITLE

SUBSONIC AERODYNAMIC STABILIZATION OF LONG, LOW-DRAG BODIES OF REVOLUTION USING BOATTAIL FINS

4. DESCRIPTIVE NOTES (Type of report and inclusive dates)

5. AUTHOR(S) (First name, middle initial, last name)

Roy W. Kline

6. REPORT DATE	7a. TOTAL NO. OF PAGES 67	7b. NO. OF REFS 18
8a. CONTRACT OR GRANT NO. b. PROJECT NO. c. AMCMS Code 554B.12.51509.02 d.	9a. ORIGINATOR'S REPORT NUMBER(S) Technical Report 4307 9b. OTHER REPORT NO(S) (Any other numbers that may be assigned this report)	

10. DISTRIBUTION STATEMENT

11. SUPPLEMENTARY NOTES	12. SPONSORING MILITARY ACTIVITY

13. ABSTRACT

Subsonic three-degree-of-freedom wind tunnel tests were utilized to demonstrate the dynamic instability of a five and one half caliber long, spin stabilized body of revolution. A modification of this body, i.e., the addition of fins to the boattail section, is shown to be an effective means of controlling this instability. The optically acquired angular orientation data was fitted to a closed form solution of the differential equations of motion. The pitching, damping, and Magnus moments were evaluated as both linear and nonlinear functions of angle of attack. The airflow over the model was observed by means of smokeflow photography.

DD FORM 1 NOV 68 1473 REPLACES DD FORM 1473, 1 JAN 64, WHICH IS OBSOLETE FOR ARMY USE.

UNCLASSIFIED
Security Classification

14. KEY WORDS	LINK A		LINK B		LINK C	
	ROLE	WT	ROLE	WT	ROLE	WT
Exterior ballistics						
Finned boattail						
Projectile						
Wind tunnel testing						
Dynamic stability						
Notre Dame						
Subsonic stabilization						
Low-drag bodies of revolution						
Boattail fins						

Technical Report 4307

SUBSONIC AERODYNAMIC STABILIZATION OF LONG, LOW-DRAG BODIES OF REVOLUTION USING BOATTAIL FINS

by

Roy W. Kline

June 1972

Approved for public release; distribution unlimited

AMCMS Code 554B.12.51509.02

Engineering Sciences Division
Feltman Research Laboratory
Picatinny Arsenal
Dover, N. J.

The citation in this report of the trade names of commercially available products does not constitute official indorsement or approval of the use of such products.

FOREWORD

This report was originally submitted to the Graduate School of the University of Notre Dame in partial fulfillment of the requirements for the degree of Master of Science.

TABLE OF CONTENTS

Tables

Figures

NOMENCLATURE

C_M — Pitching moment coefficient

$$C_M = \frac{M}{QSd}$$

C_{M_α} — Pitching moment coefficient derivative (rad^{-1})

$$C_{M_\alpha} = \frac{\partial C_M}{\partial \alpha} = \frac{M_\alpha}{\alpha QSd}$$

C_{M_q} — Damping moment coefficient derivative (rad^{-1})

$$C_{M_q} = \frac{\partial C_M}{\partial \left(\frac{qd}{2V}\right)} = \frac{M_q q}{\left(\frac{qd}{2V}\right) QSd}$$

$C_{M_{\dot\alpha}}$ — Lag moment coefficient derivative (rad^{-1})

$$C_{M_{\dot\alpha}} = \frac{\partial C_M}{\partial \left(\frac{\dot\alpha d}{2V}\right)} = \frac{M_{\dot\alpha} \dot\alpha}{\left(\frac{\dot\alpha d}{2V}\right) QSd}$$

$C_{M_{p\alpha}}$ — Magnus moment coefficient derivative (rad^{-2})

$$C_{M_{p\alpha}} = \frac{\partial^2 C_N}{\partial \alpha \, \partial \left(\frac{pd}{2V}\right)} = \frac{N_{P\alpha} P\alpha}{\left(\frac{pd}{2V}\right) \alpha QSd} = \frac{M_{P\beta} P\beta}{\left(\frac{pd}{2V}\right) \beta QSd}$$

C_{Z_α} — Normal force coefficient derivative (rad^{-1})

d — Reference length = projectile caliber (ft)

g — Acceleration due to gravity (ft/sec^2)

I — Transverse moment of inertia ($slug\text{-}ft^2$)

X

I_x	Axial moment of inertia (slug-ft^2)
i	$\sqrt{-1}$
K_N	Amplitude of nutation mode (degrees)
K_p	Amplitude of precession mode (degrees)
K_T	Rolling trim angle (degrees)
ℓ	Body length (ft)
p	Roll rate (rad/sec or RPM)
p, q, r	Angular velocity components (rad/sec)
b	Total span of the fins
P	$\frac{pd}{2V}$ nondimensional roll rate
$\frac{qd}{2V}$	Nondimensional pitching velocity
$\vec{q}$	Complex pitching velocity (rad/sec) $\vec{q} = q + ir$
Q	Dynamic pressure, $1/2\ \rho\ V^2$(lb/ft^2)
s_g	Gyroscopic stability factor
S	Reference area, $\frac{\pi d^2}{4}$ (ft^2)
t	Time (sec)
u, v, w	Transverse velocity components (ft/sec)
x, y, z	Coordinates (ft)
X_i	Distance from the nose to the center of gravity (ft)
y'	Distance from the center of the body to a chordwise strip on the fin

V	Total velocity (ft/sec)
Z	Normal force (lb)
α	Angle of attack (deg or rad)
$\vec{\alpha}$	Complex angle of attack (deg or rad)
	$\vec{\alpha} = \beta + i\alpha$
β	Angle of sideslip (deg or rad)
$\lambda_{N,p}$	Nutation and precession dynamic damping factors of linear aeroballistic theory (sec^{-1})
$\lambda^{V}_{N,p}$	Nutation and precession damping factors due to varying motion frequency (sec^{-1})
$\lambda^{*}_{N,p}$	$\lambda^{*}_{N,p} = \lambda_{N,p} + \lambda^{V}_{N,p}$
ρ	Air density ($slugs/ft^3$)
$\omega_{N,p}$	Nutation and precession frequencies (rad/sec)
τ	Dynamic weight factor
$(\ )_o$	Linear term
$(\ )_2$	Nonlinear term
(f)	Fins
α_M	Mean angle of attack $\sqrt{K_N^2 + K_p^2}$, (deg)
δ	Fin incidence angle (deg)
δ_e	Aerodynamic symmetry angle (rad or deg) e.g., an elevator deflection

θ	Angle of pitch (deg or rad)
$\vec{\theta}$	Complex pitch angle (deg or rad) $\vec{\theta} = \theta + i\varphi$
φ	Angle of yaw (deg or rad)
ϕ	Damping parameter defined by Equation 17
η_r	Yaw of repose (rad)

Superscript

$(\dot{})$	Indicates differentiation with respect to time

ABSTRACT

Subsonic three-degree-of-freedom wind tunnel tests were utilized to demonstrate the dynamic instability of a five and one half caliber long, spin stabilized body of revolution. A modification of this body, i.e., the addition of fins to the boattail section, is shown to be an effective means of controlling this instability. The optically acquired angular orientation data was fitted to a closed form solution of the differential equations of motion. The pitching, damping, and Magnus moments were evaluated as both linear and nonlinear functions of angle of attack. The airflow over the model was observed by means of smokeflow photography.

INTRODUCTION

To increase the range of a projectile one commonly increases the ballistic coefficient, i.e., the ratio of weight to the product of drag coefficient and cross sectional area. Thus, long, boattailed projectiles such as the subject of this study, shown in Figure 1, have evolved. In some cases, particularly at subsonic velocities, flight instabilities have resulted in short range and poor accuracy, necessitating the high ballistic coefficient design to be abandoned.

Increasing the length of a projectile tends to separate the center of pressure of the normal force and the center of gravity, thereby increasing the pitching moment and thus making the projectile more difficult to stabilize gyroscopically. Boattailing further aggravates this situation by moving the center of pressure further forward on the projectile. The damping moment is decreased by boattailing (Ref 8), allowing the Magnus moment to undamp the nutational mode of motion.

The prime purpose of this report is to demonstrate that vanes or fins on the boattail of this type projectile can prevent nutation instability. Both linear and nonlinear aerodynamic coefficients of the body of revolution and the body modified by the addition of the boattail fins were obtained from three degrees of freedom subsonic vertical wind tunnel testing. A total of 63 qualitative and quantative test runs was conducted at nondimensional spin rates from 0.22 to 0.45 at a wind tunnel velocity of 50 feet per second.

AEROBALLISTIC THEORY

The coefficients of the differential equations of angular motion of the wind tunnel models were extracted both as linear and nonlinear functions of angle of attack utilizing aeroballistic theory (Ref 1).

Linear Theory

For linear variations with angle of attack the aerodynamic moments can be written as

$$M + iN = -M_{\alpha}\vec{\alpha} + M_{q}\vec{q} - iM_{\dot{\alpha}}\vec{\dot{\alpha}} - PM_{p\alpha}\vec{\alpha} - iM_{\delta_e}\delta_e e^{ipt} \qquad (1)$$

The resulting complex differential equation of motion is

$$\vec{\ddot{\alpha}} - \left[\frac{iPI_x}{I} + \frac{M_q + M_{\dot{\alpha}}}{I}\right]\vec{\dot{\alpha}} - \left[\frac{M_{\alpha}}{I} + iP\frac{M_{p\alpha}}{I}\right]\vec{\alpha} = \frac{iM_{\delta_\epsilon}\delta_\epsilon}{I}e^{ipt} \qquad (1a)$$

The solution to this equation assuming constant velocity and roll rate is found to be

$$\theta = K_N e^{(\lambda_N + i\omega_N)t} + K_P e^{(\lambda_p + i\omega_p)t} + K_T e^{ipt} \qquad (2)$$

where

$$\lambda_{N,p} = \frac{QSd^2}{2V}\left[\frac{C_{M_q} + C_{M_{\dot{\alpha}}}}{2I}(1 + \gamma) \pm C_{M_{p\alpha}}\frac{\gamma}{I_x}\right] \qquad (3)$$

$$\omega_{N,p} = \frac{pI_x}{2I}\left(1 \pm \frac{1}{\gamma}\right) \qquad (4)$$

$$\gamma = \frac{1}{(1 - 1/s_g)^{1/2}} \qquad (5)$$

$$s_g = \frac{(I_x p)^2}{4I\, C_{M_\alpha} QSd} \qquad (6)$$

$$K_T = \frac{C_{M_{\delta\epsilon}} \delta_\epsilon QSd}{I\left[i\,(p-\omega_N) - \lambda_N\right]\left[\,i(p-\omega_p) - \lambda_p\,\right]} \tag{7}$$

Nonlinear Theory (Ref 1, 2, 3)

If the aerodynamic moments are assumed to be nonlinear functions of the complex angle of attack, then

$$-(M + iN) = M_\alpha(|\vec{\alpha}|)\,\vec{\alpha} + M_q(|\vec{\alpha}|)\,\vec{\alpha} + M_{\dot{\alpha}}(|\vec{\alpha}|)\,\vec{\alpha} + M_{P\alpha}(|\vec{\alpha}|)P\,\vec{\alpha} \tag{8}$$

where

$$M_\alpha(|\alpha|) = M_{\alpha_o} + M_{\alpha_2}|\vec{\alpha}|^2 \tag{9}$$

$$M_q(|\alpha|) = M_{q_o} + M_{q_2}|\vec{\alpha}|^2 \tag{10}$$

$$M_{\dot{\alpha}}(|\alpha|) = M_{\dot{\alpha}_o} + M_{\dot{\alpha}_2}|\vec{\alpha}|^2 \tag{11}$$

$$M_{P_\alpha}(|\alpha|) = M_{P_{\alpha o}} + M_{P_{\alpha 2}}|\vec{\alpha}|^2 \tag{12}$$

The nonlinear theory assumes an approximate solution of the same form as the linear theory; however, the stability parameters now contain a nonlinearity in the form of a second order term.

The solution for the complex angle of attack is given by (Ref 1, 2):

$$\theta = K_N e^{i\phi_N t} + K_p e^{i\phi_p t} \tag{13}$$

$$\vec{\theta} = \theta + i\psi \tag{14}$$

$$K_N = K_{N_o} e^{\lambda^*_N t}, \quad K_p = K_{p_o} e^{\lambda^*_p t} \tag{15}$$

$$\lambda^*_{N,p} = \lambda_{N,p} + \lambda^v_{N,p} \tag{16}$$

$$\lambda_{N,p} = \frac{QSd^2}{2V}\left[\frac{(C_{M_q} + C_{m_{\dot{\alpha}}})}{2I}(1 \pm \tau_{N,p}) \pm \frac{(C_{M_{p\alpha}} + C_{M_{p\alpha}}\delta_{eN}^2)}{I_x}\tau_{N,p}\right] + \frac{(C_{M_q} + C_{M_{\dot{\alpha}}})_2}{2I}$$

$$\left[(1 \pm \tau_{N,p})(K_{N,p}^2 + K_{p,N}^2) + K_{p,N}^2 \tau_{N,p}(-\tau_{p,N} \pm 1)\right] \tag{17}$$

$$\lambda'_{N,p} = \frac{QSd^2}{2V}\left[\frac{2IV}{d(pI_x)^2}\, C_{M_{\alpha 2}}\, \tau_{N,p}^2\, (K_{N,p}\dot{K}_{N,p} + 2K_{,N}\dot{K}_{,N})\right] \tag{18}$$

$$\lambda^*_{N,p} = \frac{QSd^2}{2V}\left\{\left[\frac{IV}{2d\,p^2 I_x^2}\, C_{M_{\alpha 2}}\, (K_{N,p}\dot{K}_{N,p} + 2K_{N,p}\dot{K}_{p,N})\, \tau_{N,p}^2\right]\right.$$

$$+ \frac{(C_{M_q} + C_{M_{\dot{\alpha}}})_o}{2I}\,(1 \pm \tau_{N,p}) \pm \frac{(C_{M_{p\alpha o}} + C_{M_{p\alpha 2}}\,\delta^2_{\epsilon_N})}{I_\lambda}\,\tau_{N,p}$$

$$\left. + \frac{(C_{M_q} + C_{M_{\dot{\alpha}}})_2}{2I}\left[(1 \pm \tau_{N,p})(K^2_{N,p} + K^2_{p,N}) + K^2_{p,N}\,\tau_{N,p}(-\tau_{p,N} \pm 1)\right]\right\} \tag{19}$$

$$\phi_{N,p} = \frac{pI_x}{2I}\left(1 \pm \frac{1}{\tau_{N,p}}\right)t + \phi_{N_o p_o} \tag{20}$$

$$\omega_{N,p} = \phi_{N,p} = \frac{pI_x}{2I}\left(1 \pm \frac{1}{\tau_{N,p}}\right) \tag{21}$$

$$\tau_{N,p} = \left(1 - \frac{1}{s_{N,p}}\right)^{-1/2} \tag{22}$$

$$s_{N,p} = \frac{(pI_x)^2}{4I\left(C_{M_{\alpha o}} + C_{M_{\alpha 2}}\delta^2_{\epsilon_{N,p}}\right)QSd} \tag{23}$$

where

$$\delta^2_{\epsilon_{N,p}} = K^2_{N,p} + 2K^2_{p,N} \tag{24}$$

A frequency variation, resulting from a nonlinear restoring moment, changes in the air density, velocity, or roll rate, will cause the size of the arms of the motion to vary in the following manner (Ref 3):

$$K_{N,p}(t) = \left[\frac{\omega_{N,p}(o)}{\omega_{N,p}(t)} \right]^{1/2} K_{N,p}(o) \qquad (25)$$

Computation of Aerodynamic Coefficients

To obtain aerodynamic stability coefficients from the angular data obtained from the wind tunnel tests, the aeroballistic theory is fitted to the angular orientation data, θ , ψ . This is done through the use of the WOBBLE computer program (Ref 3). This program fits the theory to short segments of the data in overlapping sections so that the stability parameters, $K_{N,p}$, $\lambda_{N,p}$, $\omega_{N,p}$, are determined as functions of time. Since the nonlinear theory assumes an approximate solution of the same form as the linear theory, the WOBBLE program can be applied to both.

Computation of Linear Coefficients

Using $\lambda_{N,p}$ and $\omega_{N,p}$, along with the velocity, dynamic pressure, roll rate, and physical parameters of the projectile, the aerodynamic stability coefficients, C_{M_α} , $C_{M_q} + C_{M_{\dot{\alpha}}}$, and $C_{M_{p\alpha}}$, were computed as functions of time from the following equations:

$$C_{M_\alpha} = \frac{\omega_N \omega_p}{\pi \rho d^3 V^2} \qquad (26)$$

$$C_{M_q} + C_{M_{\dot{\alpha}}} = \frac{2IV}{QSd^2} (\lambda_N + \lambda_p) \qquad (27)$$

$$C_{M_{P\alpha}} = \frac{I_x}{\tau} \left[\frac{2V}{QSd^2} (\lambda_N, \lambda_p) - \frac{1}{2I} (C_{M_q} + C_{M_{\dot{\alpha}}}) (1 \pm \tau) \right] \quad (28)$$

Computation of Nonlinear Coefficients

The nonlinear aerodynamic stability coefficients, $C_{M_\alpha}(\alpha)$, $C_{M_q}(\alpha) + C_{M_{\dot{\alpha}}}(\alpha)$, and $C_{M_{P\alpha}}(\alpha)$ were computed as polynomial functions of the complex angle of attack as follows:

$$\omega_N \omega_p = \left[\frac{(C_{M_\alpha})_o}{I} + \frac{(C_{M_\alpha})_2}{I} \delta_\alpha^2 \right] QSd \quad (29)$$

$$\delta_\alpha^2 = K_N^2 + K_p^2 + \frac{K_N^2 \omega_N - K_p^2 \omega_p}{\omega_N - \omega_p} \quad (30)$$

Using a least squares technique to fit a straight line to $\omega_N \omega_p$ versus δ_α^2 yields $(C_{M_\alpha})_o$ as the intercept and $(C_{M_\alpha})_2$ as the slope.

Correcting λ_N^* and λ_p^* by determing λ_N^v and λ_p^v from a logarithmic technique developed in Reference 3, the actual damping rates λ_N and λ_p are fitted simultaneously with a least squares procedure to yield $(C_{M_q} + C_{M_{\dot{\alpha}}})_0$, $(C_{M_q} + C_{M_{\dot{\alpha}}})_2$, $(C_{M_{P\alpha}})_0$, and $(C_{M_{P\alpha}})_2$.

One must exercise great care in using these coefficients if, as in the case of this experiment, the span of data is small. The higher order coefficients may indicate a larger nonlinearity than is present if the short data set contains even a small amount of scatter. A plot of the nonlinear coefficient will always yield a satisfactory value of aerodynamic coefficient near the mean angle of attack of such a set of data and will reliably indicate the hard or soft spring nature of the coefficient, but may diverge rapidly from reality if values of the coefficient are calculated near the end or beyond the data set.

EXPERIMENTAL TECHNIQUE

The 1.95 inch diameter model used in the experimental program was 5.58 calibers in length with a 2.9 caliber double secant ogive nose and a .59 caliber, 7°: 35' boattail. The University of Notre Dame Aerospace Laboratory's extremely low friction jewel-bearing support system allowed the model to pitch, yaw and roll with negligible mechanical damping. The model is pictured in Figures 2 and 3. Figure 1 contains an externally dimensioned drawing of the model and a typical boattail fin.

Model Physical Characteristics

With the exception of a brass cylinder used to achieve an appropriate moment of inertia ratio and center of gravity location, the model was constructed of high strength aluminum. The axial and transverse moments of inertia were determined using a standard torsional pendulum technique. These values together with the model mass are listed in Table 1. The boattail fins were made from 0.01 inch aluminum sheet and attached to the base of the model at 17° cant in the right-handed direction of model spin. These fins were found to increase the mass of the model by approximately one quarter of one percent and the moments of inertia by less than one percent, which is nearly the measuring accuracy of the torsional pendulum.

The model was mounted with its center of gravity coincident with the jewel-bearing support and dynamically balanced before testing, and checked before each set of test runs on the jewel support.

Wind Tunnel Testing and Equipment (Ref 6, 8)

The dynamic stability wind tunnel tests were conducted in the University of Notre Dame's vertical-downdraft wind tunnel at a velocity of 50 feet per second. A Milliken constant speed motion picture camera recorded the angular motion of the model during each test run at a rate of 128 frames per second. Model spin was induced by passing a high velocity airstream over the side of the model. Spin rate was determined by a stroboscopic light source.

Smoke Tunnel Testing and Equipment

Smokeflow photographs of the finned and unfinned model were taken in one of the University of Notre Dame Aerospace Laboratory's horizontal two by two foot wind tunnels at the same operating conditions as the dynamic stability tests. The flow visualization equipment used in this investigation was developed by Brown (Ref 13). The smoke issues from a rake through a single tube into the nonreturn type tunnel (Fig 26). The velocity in this region is very low, of the order of one foot per second. The smoke then flows through an entrance contraction, and into the test section. A detailed description of the wind tunnel is given in Reference 6.

Data Reduction

On each frame of movie film were recorded two reference points, the center point of the model nose and roll position indicators. A schematic of typical frame is shown in Figure 6. The relative distances from point to point on each frame were measured on an optical comparitor and converted to angular orientation. Overlapping sections of this data from each test run was then fitted to the equations of aeroballistic theory, yielding the motion frequencies and damping factors. This, together with the physical parameters of the model and the test conditions, gave the coefficients of the differential equations of angular motion.

DISCUSSION OF RESULTS

The objective of the test program was to observe and record a wide variety of model motions generated with various initial angular orientations and angular velocities. Qualitative observations of model motion were made during the test, and so was a film record of the types of motion which were most amenable to fitting aeroballistic theory, i.e., motions whose two arms could be clearly defined. In all cases the gyroscopic stability factor was between two and three and one half (Ref 3, 5) as is shown in Figure 24. This is sufficiently above the limiting value of one (Ref 1).

Angular Motion of the Body of Revolution

The oscillatory motion of the body of revolution was characterized by an undamped nutation arm and a strongly damped precession arm. When K_N was initially small compared with K_p, the total motion damped, usually to half its initial size in approximately one precession cycle. With the vanishing of the precessional mode, the motion consisted solely of the rapid rotation of the undamped nutation arm. This, of course, was verified in the WOBBLE calculation of the model damping factors, λ_N and λ_p. These are plotted vs time in Figures 12 through 17. An example of this phenomenon, shown in a complex motion plot, is given in Figure 10. In several test runs the nutation arm was initially the larger component of the motion, which resulted in almost immediate divergence of the total motion.

Tests were conducted at initial roll rates from 1500 to 2500 revolutions per minute or a $\frac{pd}{2V}$ of 0.22 to 0.45. Considering that the prime area of interest in the flight of this projectile is near the trajectory apex, these spin rates would be obtained with a launcher rifling twist of one turn of the projectile in 20 calibers of linear travel at quadrant elevations of 45 to 65 degrees. Variations in roll rate had no observable effect on the damping characteristics, but resulted only in the expected changes in the motion frequencies. As Figure 24 indicates, decreasing the gyroscopic stability factor lowers the nutation damping factor.

Body of Revolution Stability Parameters

The parameters of aeroballistic theory, the size, frequency, and damping factors of the nutation and precession modes, were fit to the photographically recorded angular motion utilizing the WOBBLE computer program (Ref 3). In all cases the probable error of fit was less than one tenth of one degree. The results, which were in agreement with observations from many qualitative test runs, were obtained from three of the data sets in which more than one and one-half precession cycles could be discerned. The precession damping factor was found to average 0.25 per second, indicating an average half life of this arm of less than three seconds (or 0.8 cycles). The unstable nutation arm more than doubled its size every three and one-half seconds (or 9.5 cycles).

As Figures 12, 13, and 14 indicate, the motion arms and thus their damping factors did not change as a linear function of time. This is due to the nonlinearity of the Magnus and damping moments in angle of attack, and also to the size of the measurement error compared with the initially small nutation arm; and finally, at the end of the data, the disappearance of the precession arm. The nutation frequency decreased slightly while the precession frequency remained nearly constant. This indicates the very mild stiffening of the pitching moment in angle of attack brought about by the appearance of the boattail section in the flow. This very moderate hard-spring nature of the static moment was found to have a negligible effect on the damping rates (Ref 2, 3). The pitching moment calculated by nonlinear aeroballistic theory and plotted in Figure 25 was found to be very nearly constant.

The damping and Magnus moment coefficients calculated from succeeding sections of data varied only by a small amount with time (Fig 18, 19, 20). The hard-spring nature of these moments, found from nonlinear aeroballistic theory, was not readily apparent in these plots, since the total angle of attack initially decreased to half its size, but subsequently grew again, due to the divergent nutation arm. The hard-spring trend of the Magnus moment (Fig 25) is due to the formation of an asymmetrical vortex pattern along the lee side of the body.

The Effect of Boattail Fins on the Angular Motion

Following the recording of the angular motion, the small boattail fins were mounted on the boattail section of the model at the extreme aft position. In all 23 qualitative test runs and 15 recorded sets of data with the finned body, both motion arms damped. After a period of nearly 25 seconds, angular motion was no longer observable. No rolling trim angle could be detected due to boattail fin mass unbalance or malalignment. Figure 11 is a complex plot of the motion of the body with boattail fins, observed in a typical test run.

Boattail Finned Body Stability Parameters

The addition of boattail fins to the body of revolution nearly doubled the damping moment and diminished, by approximately 20 percent, the Magnus moment, yielding a more appropriate balance of these moments for dynamic stability.[1] The precession arm damping was lessened by a small amount by this rearrangement of the aerodynamics, its motion half life was now approximately three and one half seconds (or 1.1 cycle). The nutation arm, rather than rapidly diverging, was found to be lightly damped, the half life being seven seconds (or 16.7 cycles). As the size of the arms decreased to the area where $K_N + K_D < 3°$, the nutation damping factor, approached, but never reached, zero, indicating the possibility of limit cycle motion if smaller, fewer, or less effective fins were utilized. A comparable decrease in the precession damping factor was observed, as was to be expected. The motion frequencies, and especially the precession frequency, were found to be less linear in time than those of the body of revolution. This had nothing to do with the spin rate which was observed to vary only ten revolutions per minute or one half of one percent over a seven and one-half second test run of either the body of revolution per se, or the body of revolution with boattail fins.

Plots from both the linear and nonlinear aeroballistic theory (Fig 21, 22, 23, 25) indicate that the pitching moment has a very mild soft-spring tendency. Such a trend was unexpected, but may be explained by the fact that, as angle of attack increases, the two or three lee side boattail fins are washed out, while at very low angles of attack they are lifting.

---

[1] A theoretical estimate of the effectiveness of the boattail fins is made in the Appendix

The Magnus moment coefficient also exhibited a mild soft-spring trend in angle of attack as is indicated in Figures 21, 22, 23, and 25. The hard-spring nature of the damping moment found from nonlinear aeroballistic theory appears to have been tempered by the addition of boattail fins, probably due to the same phenomenon that softened the pitching moment.

The addition of boattail fins to a free flight projectile will cause the nondimensional spin rate to approach 0.3. Since the typical launch $\frac{pd}{2V}$ of this type projectile without boattail fins is 0.15, the nondimensional spin rate will increase throughout the greater part of the trajectory, and the gyroscopic stability factor will approach 2.3. The effect of $\frac{pd}{2V}$ on projectile range and deflection can be inferred from calculation of the yaw of repose at trajectory apex:

$$\zeta_r = \frac{4 g I_x}{\rho S C_{M_\alpha} V^2} \left[\frac{pd}{2V} + 2i \frac{C_{M_{p\alpha}}}{C_{M_\alpha}} \left(\frac{pd}{2V} \right)^2 \right] \quad (31)$$

CONCLUSIONS AND RECOMMENDATIONS

Boattail fins have been shown to be an effective means of dynamically stabilizing a long boattailed body of revolution at low subsonic velocities. Their application should lead to the successful flight of five and one half caliber, and longer, higher ballistic coefficient bodies in this flight range.

The body of revolution was observed to be dynamically unstable over a wide range of spin rates. The parameters of aeroballistic theory and the stability coefficients extracted from the three degree of freedom angular motion clearly defined the problem as a nutation instability. This was due to the improper balance of the Magnus and damping moments. By nearly doubling the damping moment and decreasing the Magnus moment through the use of the boattail fins, the nutation mode was damped.

The use of an extremely low friction mounting system in the low turbulence wind tunnel and the recording of the angular position of the model 50 times per nutation cycle yielded excellent repeatability of the linear aerodynamic coefficients and a good indication of the nonlinear nature of the aerodynamic stability coefficients.

Further aerodynamic testing should be conducted to ascertain the effect of lower spin rate, movement of center of gravity location, changes in the moments of inertia, variation of Reynolds number, and other methods of modifying the aerodynamic characteristics. Since this type body is generally designed for supersonic as well as subsonic flight, three degree of freedom testing should be conducted at supersonic and transonic velocities.

The estimated increase in drag due to the presence of boattail fins (Ref 14) was found to be small compared with the drag reduction gained by boattailing. The smokeflow photographs (Fig 26 and 27) would appear to support this conclusion. It should, however, be corroborated by free flight measurements.

REFERENCES

1. Nicolaides, J. "Free Flight Dynamics," Text, Aero-Space Engineering Department, University of Notre Dame, 1961

2. Ingram, C., "On Obtaining Nonlinear Aerodynamic Stability Coefficients from the Free Angular Motions of Rigid Bodies," Doctoral Dissertation, Department of Aero-Space Engineering, University of Notre Dame, 1969

3. Eikenberry, R., "Analysis of the Angular Motion of Missiles," Sandia Report SC-CR-70-6051, Sandia Laboratories, Albuquerque, New Mexico, 1970

4. Milne-Thompson, L., Theoretical Aerodynamics, The Mac-Millan Co., New York, 1948

5. Sacks, A. "Aerodynamic Forces, Moments and Stability Derivatives for Bodies of General Cross-section," National Advisory Committee for Aeronautics Technical Note 3283, June 1954

6. Cormier, D. and Noethen, T., "Three Dimensional Wind Tunnel Testing Technique," University of Notre Dame Report, 1969

7. Munk, M., "The Aerodynamic Forces on Airship Hulls," National Advisory Committee for Aeronautics Technical Report 184, 1924

8. MacAllister, L., Kline, R., and Gazdayka, W., "The Effect of a Subcaliber Cylindrical After-Body on the Behavior of Spin Stabilized Projectiles," American Institute of Aeronautics and Astronautics Paper No. 70-558, May 1970

9. Nicolaides, J. D., "A History of Ordnance Flight Dynamics," American Institute of Aeronautics and Astronautics Paper No. 70-533, May 1970

10. Murphy, C., "Free Flight Motion of Symmetric Missiles," Ballistic Research Laboratories Technical Report 1216, July 1963

11. Zaroodny, S., "A Simplified Approach to the Yawing Motion of a Spinning Shell," Ballistic Research Laboratories Technical Report 921, August 1954

12. Chadwick, W. and Sylvester, J., "Dynamic Stability of the 5-Inch-38 Rocket Assisted Projectile," U. S. Naval Weapons Laboratory Technical Report K-63/66, November 1966

13. Brown, F.N.M., "See the Wind Blow," Published by the author, Ostemo Place, South Bend, Indiana, 1971

14. Hitchcock, H., "On Estimating the Drag Coefficient of Missiles," Ballistic Research Laboratories Technical Report 545, May 1951

15. Laitone, E., "The Subsonic Flow About a Body of Revolution," Quarterly of Applied Math. Vol. V, No. 2, 1950

16. Dunn, E. and Hauer, H., "Theoretical Aerodynamic Characteristics of a Body of Revolution with Parabolic Head and Boattail Sections," U. S. Naval Ordnance Test Station Report Technical Memorandum 992, May 1953

17. Allen, H. and Perkins, E., "A Study of the Effects of Viscosity on Flow over Slender Inclined Bodies of Revolution, National Advisory Committee for Aeronautics Technical Report 1048, 1951

18. Perkins, C. and Hage, R., Airplane Performance Stability and Control, John Wiley and Sons Incorporated, 1949

TABLE 1

Physical characteristics of the model

Reference diameter, ft	.1625
Length, calibers	5.58
Mass, slugs	.02
Axial moment of inertia, slug-ft^2	.000092
Transverse moment of inertia, slug-ft^2	.00102

TABLE 2

Summary of the linear aerodynamic coefficients from the body of revolution

(Mean Values)

Run No.	Spin Rate (rad/sec)	C_{M_α} per rad	$C_{M_q} + C_{M_{\dot{\alpha}}}$ per rad	$C_{M_{p\alpha}}$ per rad^2
5C	220	3.05	-12.5	1.80
13A	180	3.07	-12.2	2.01
17A	180	3.08	-12.8	1.80

TABLE 3

Summary of the linear aerodynamic coefficients from the body with boattail fins

(Mean Values)

Run No.	Spin Rate (rad/sec)	C_{M_α} per rad	$C_{M_q} + C_{M_{\dot{\alpha}}}$ per rad	$C_{M_{p\alpha}}$ per rad^2
22B	185	2.77	-23.3	1.72
22C	170	2.82	-26.6	1.50
24C	188	2.73	-20.4	1.58

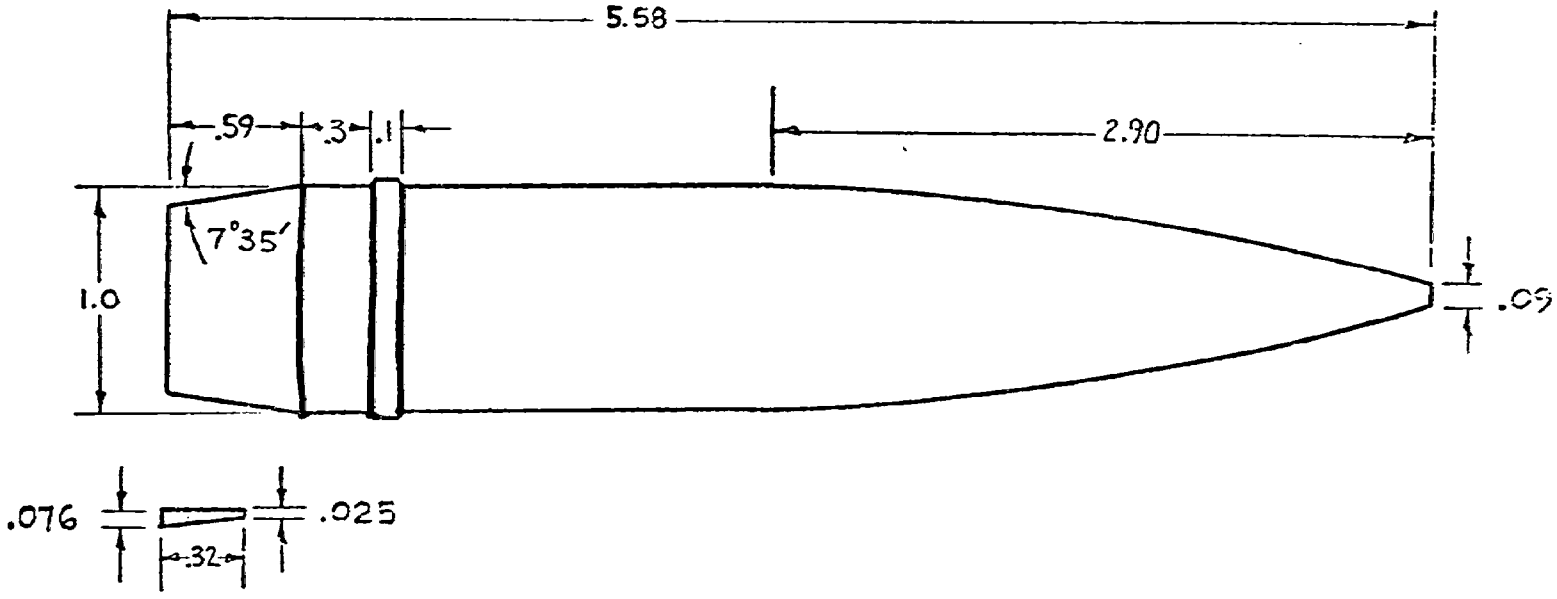

All Dimensions in Calibers

Fig 1 Wind tunnel model and typical boattail fin

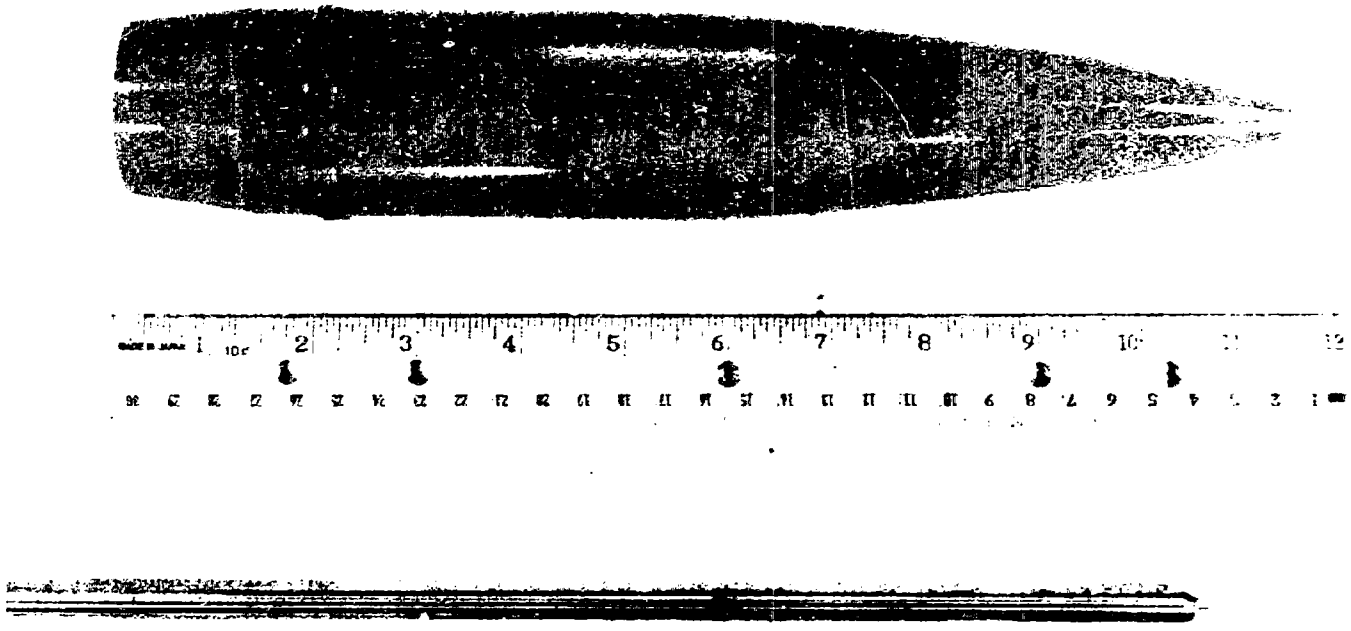

Fig 2 Body of revolution model

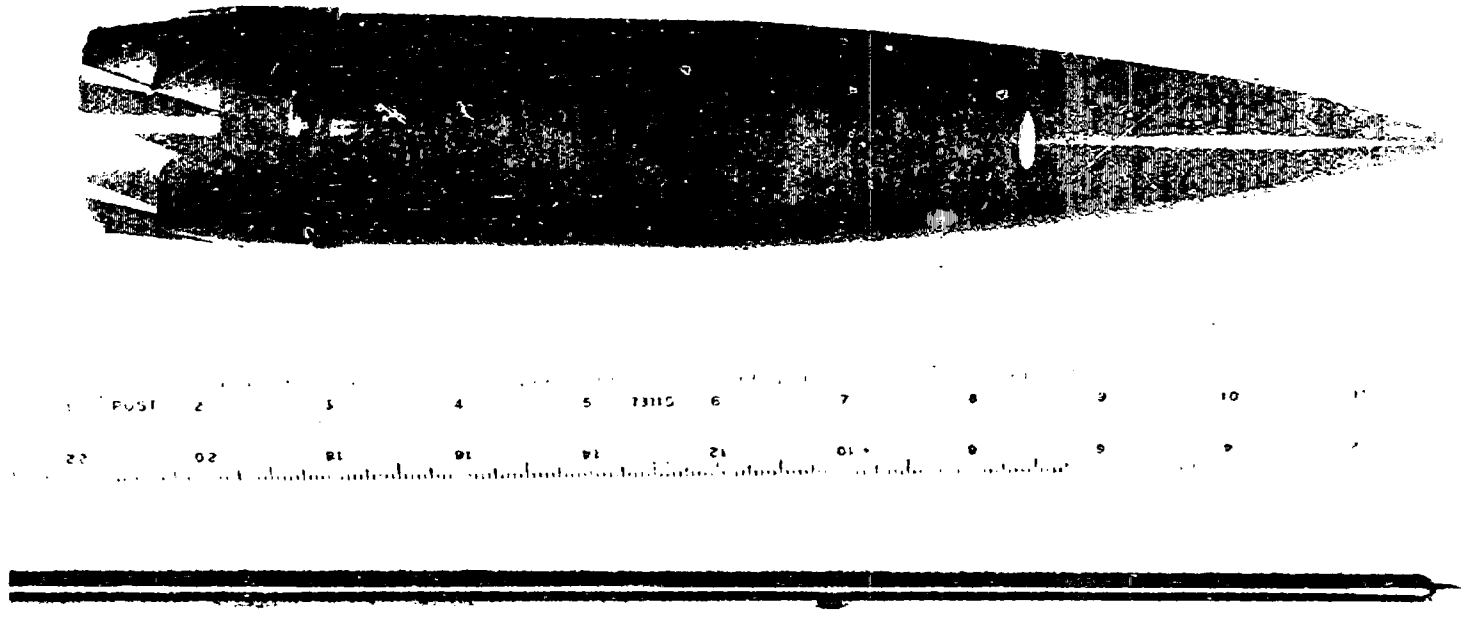

Fig 3 Model with boattail fins

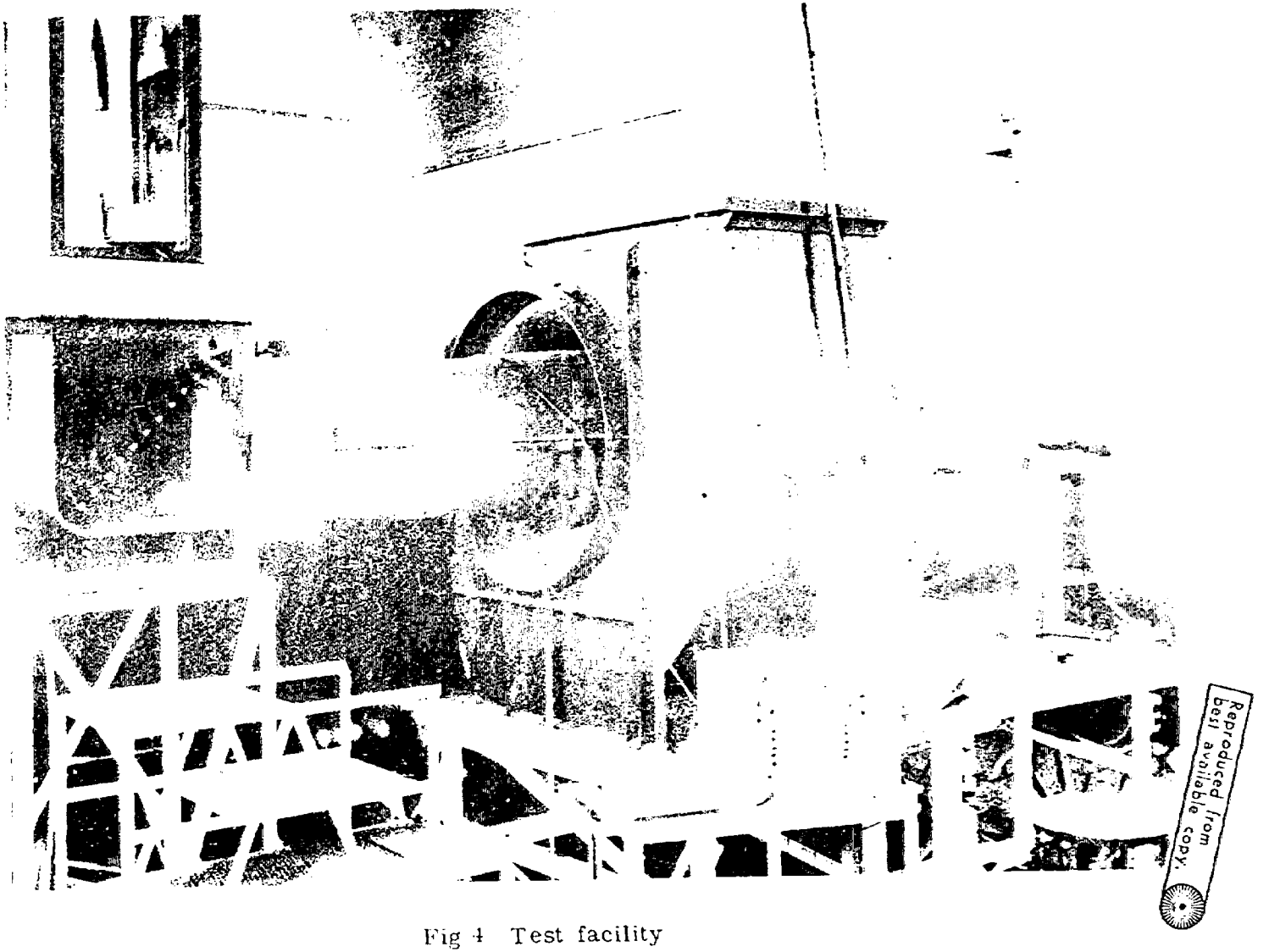

Fig 4 Test facility

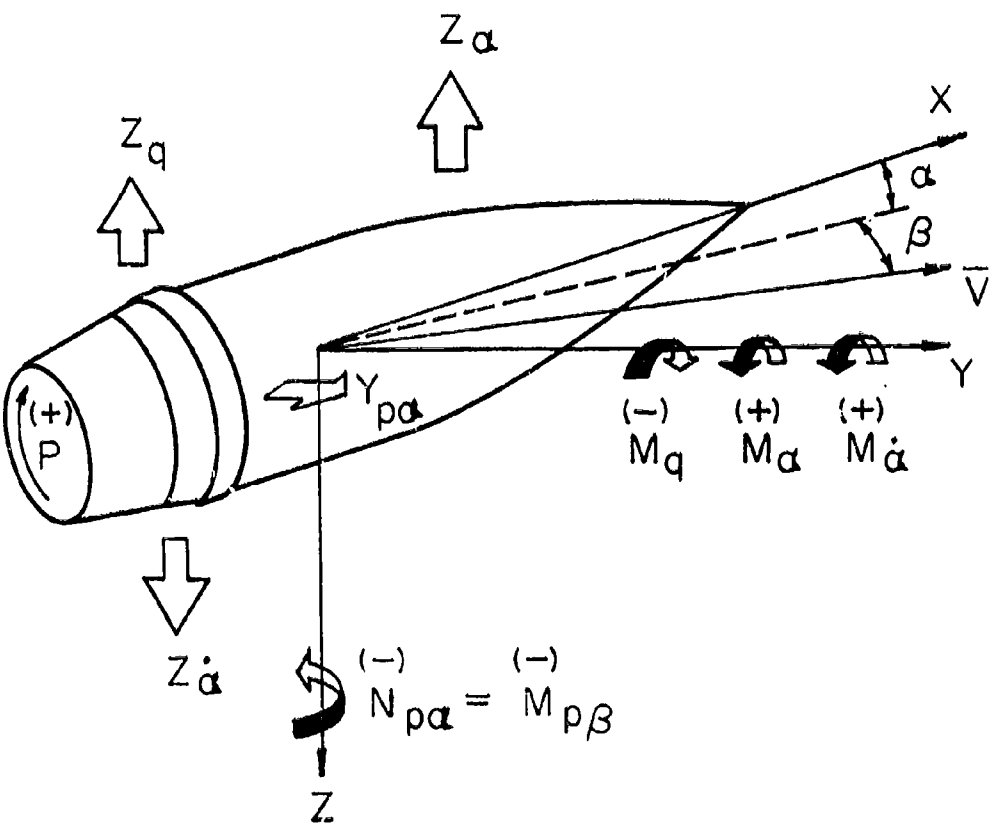

Fig 5 Aerodynamic forces and moments

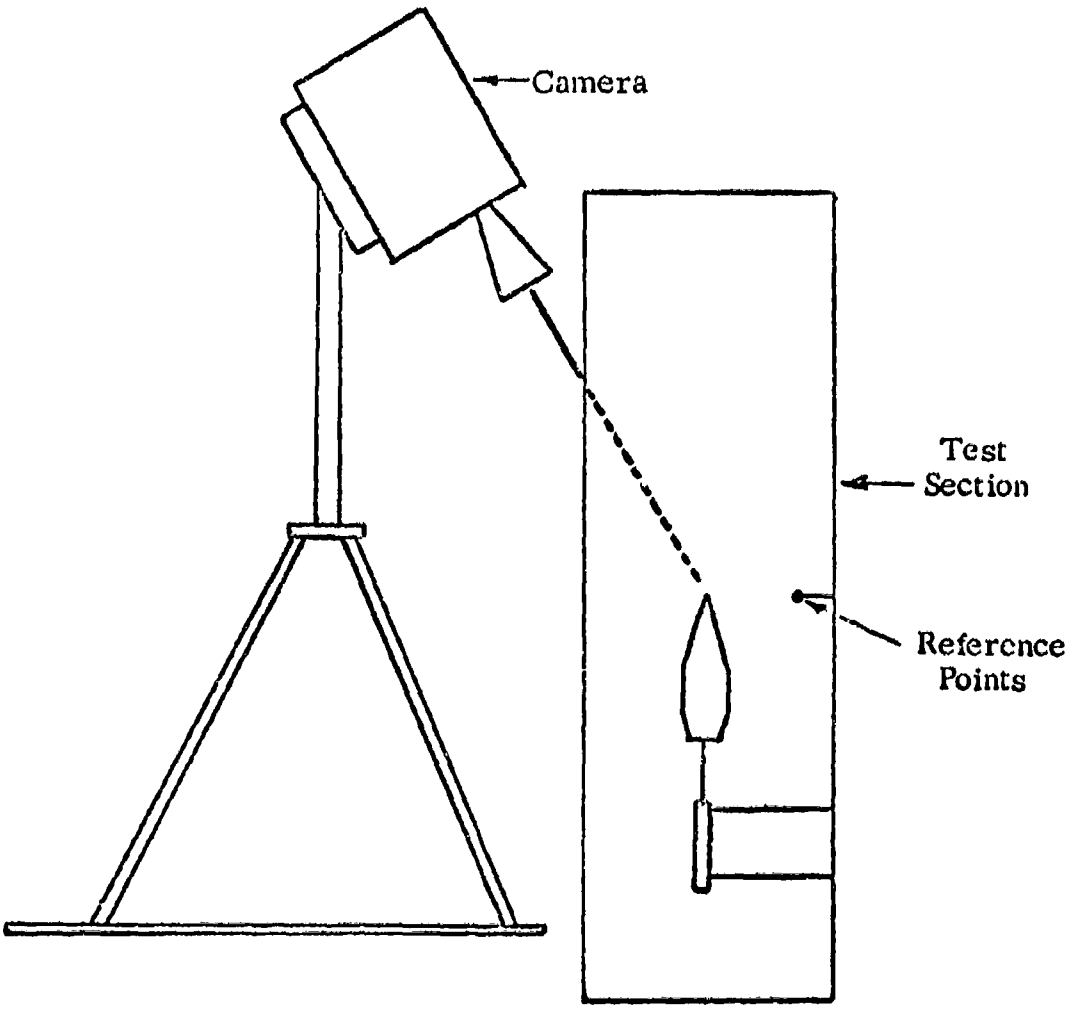

Fig 6 Position of test equipment

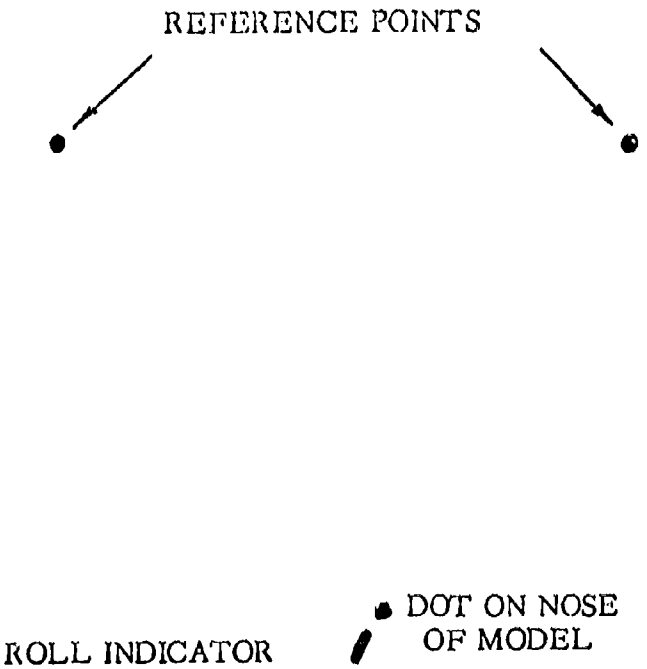

Fig 7 Sample data frame

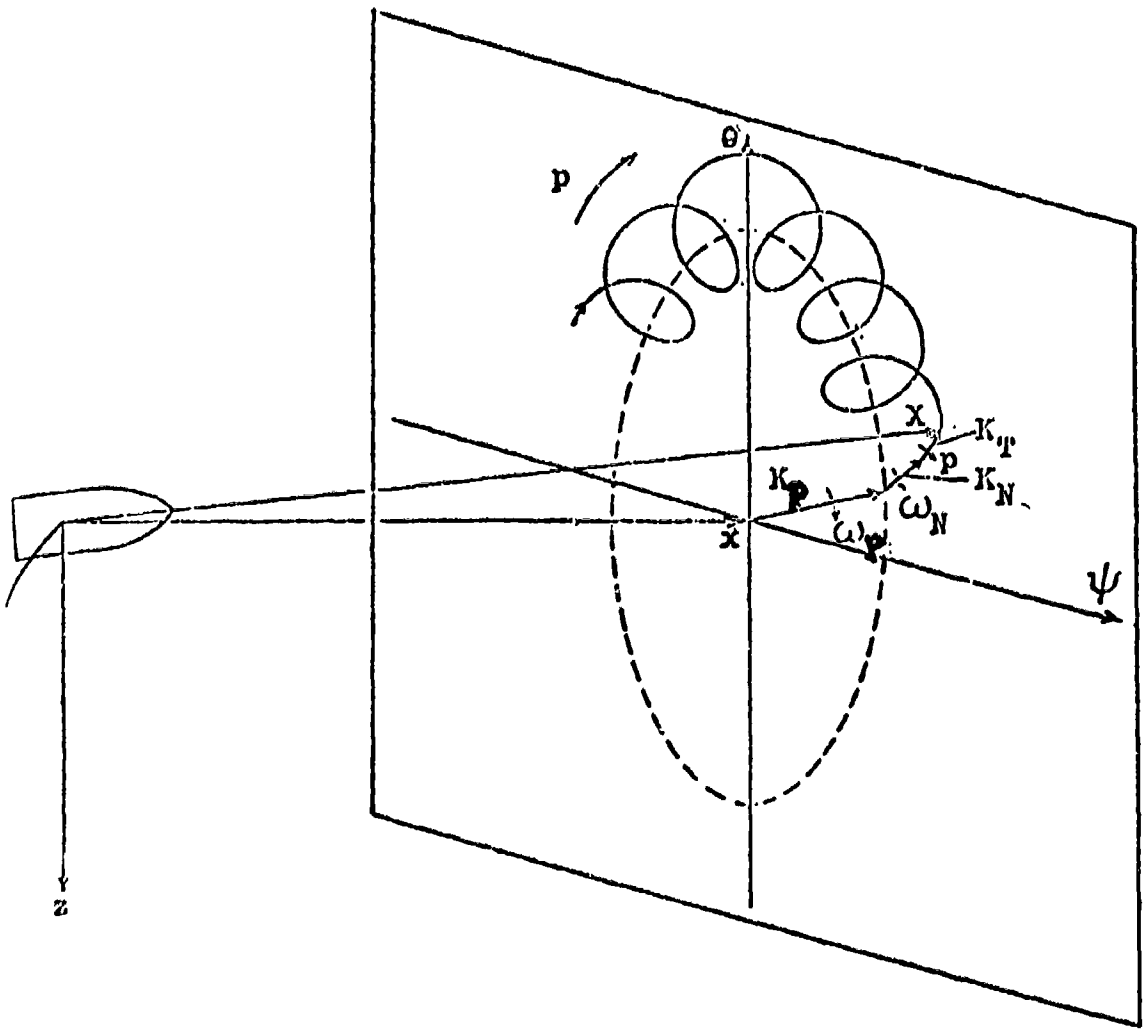

Fig 8 Tricyclic motion

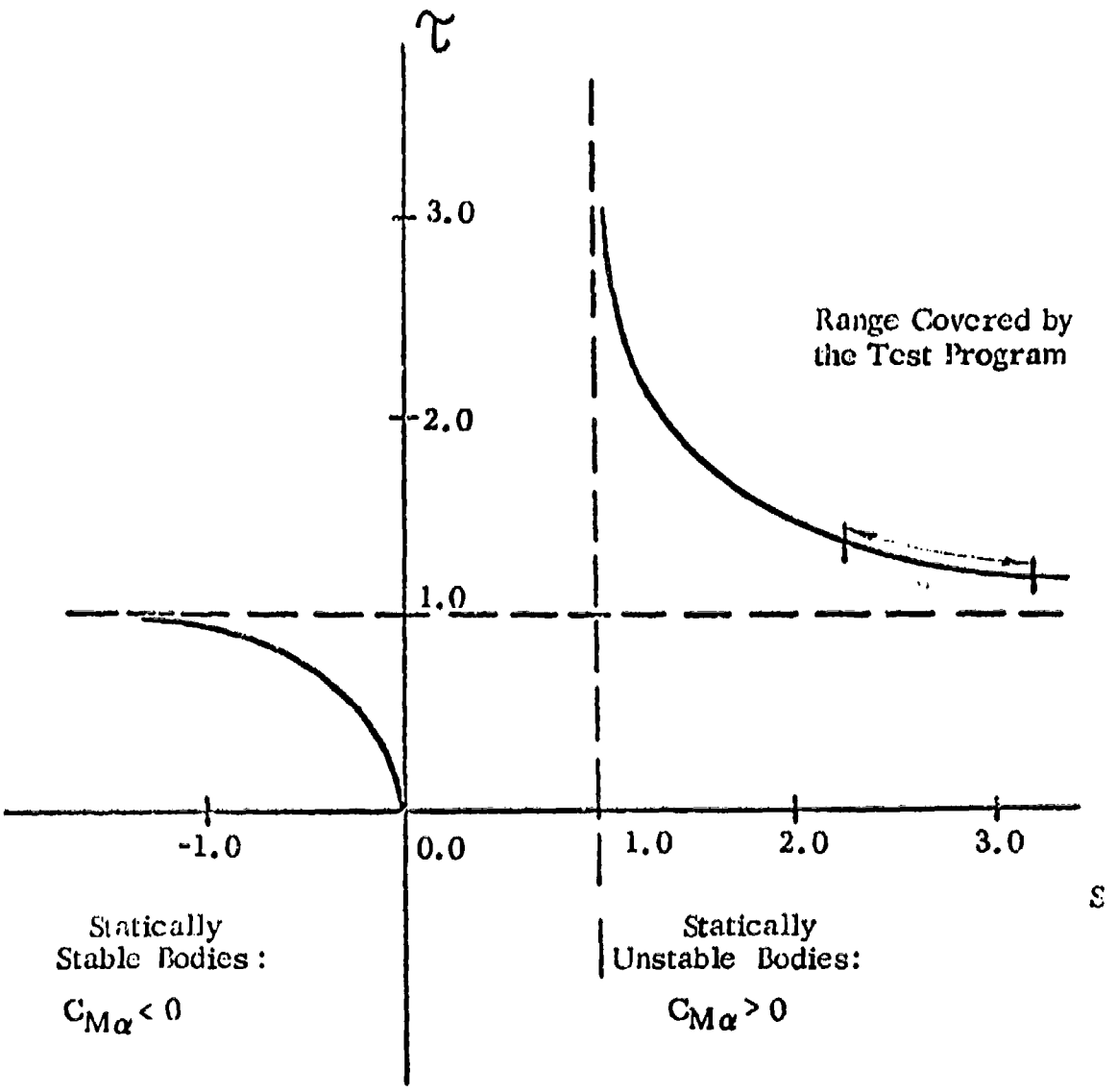

Fig 9 Dynamic weight factor τ vs gyroscopic stability factor s_g

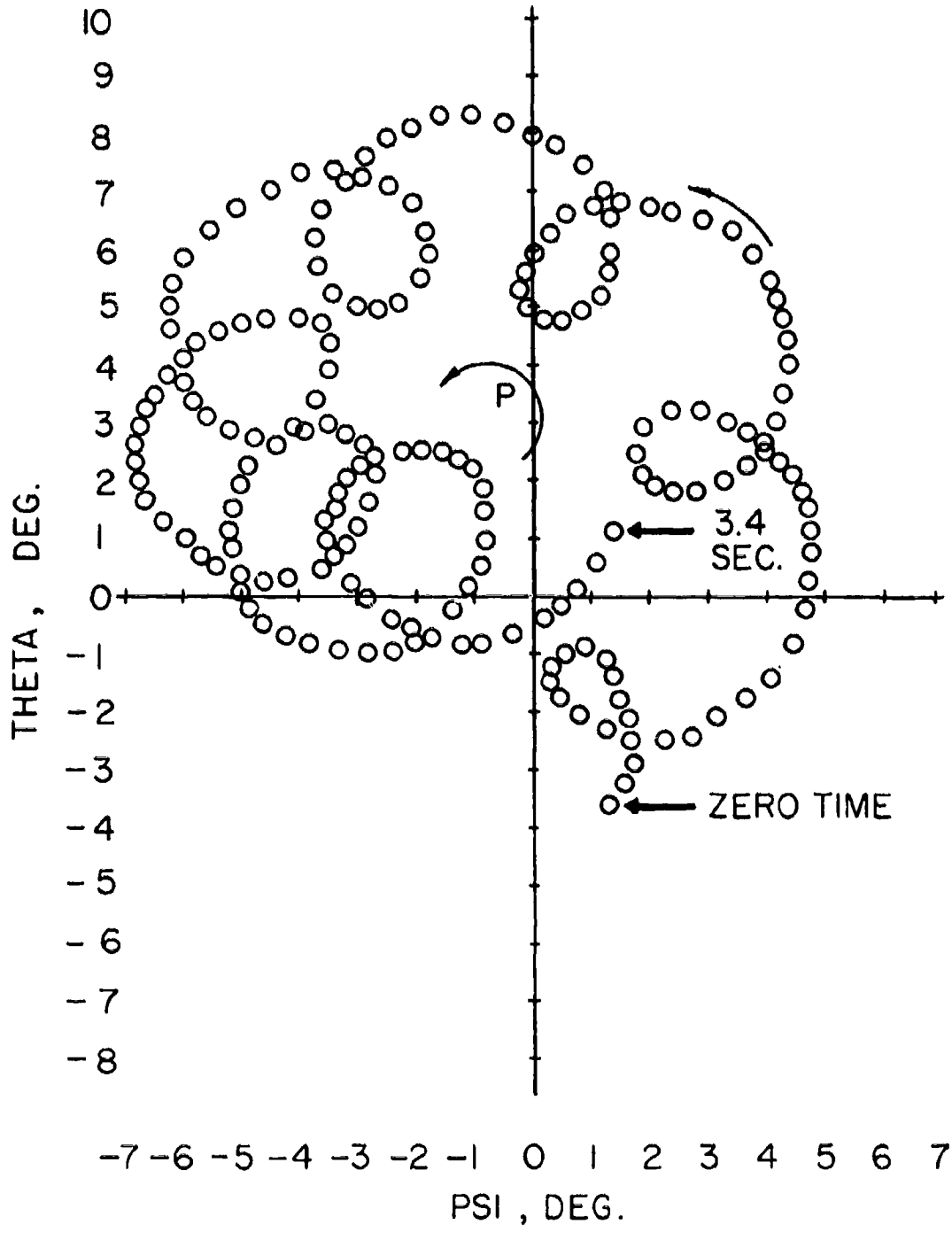

Fig 10 Typical plot of complex angular motion of body of revolution (Run 17A, 0.0 to 6.13 seconds)

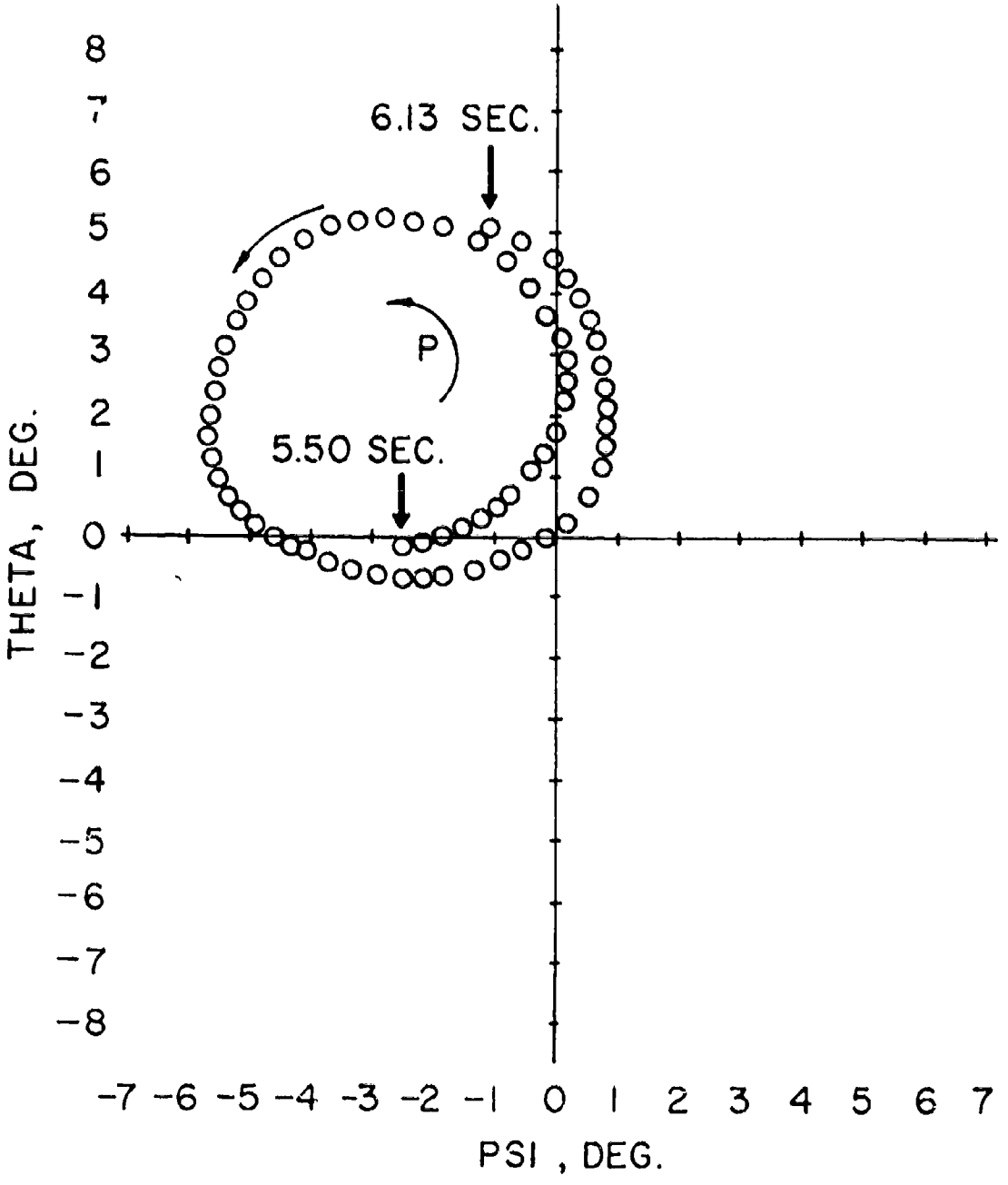
6.13 SEC.
5.50 SEC.
P
THETA, DEG.
PSI , DEG.
8
7
6
5
4
3
2
1
0
-1
-2
-3
-4
-5
-6
-7
-8
-7 -6 -5 -4 -3 -2 -1 0 1 2 3 4 5 6 7

Fig 10 (Cont'd)

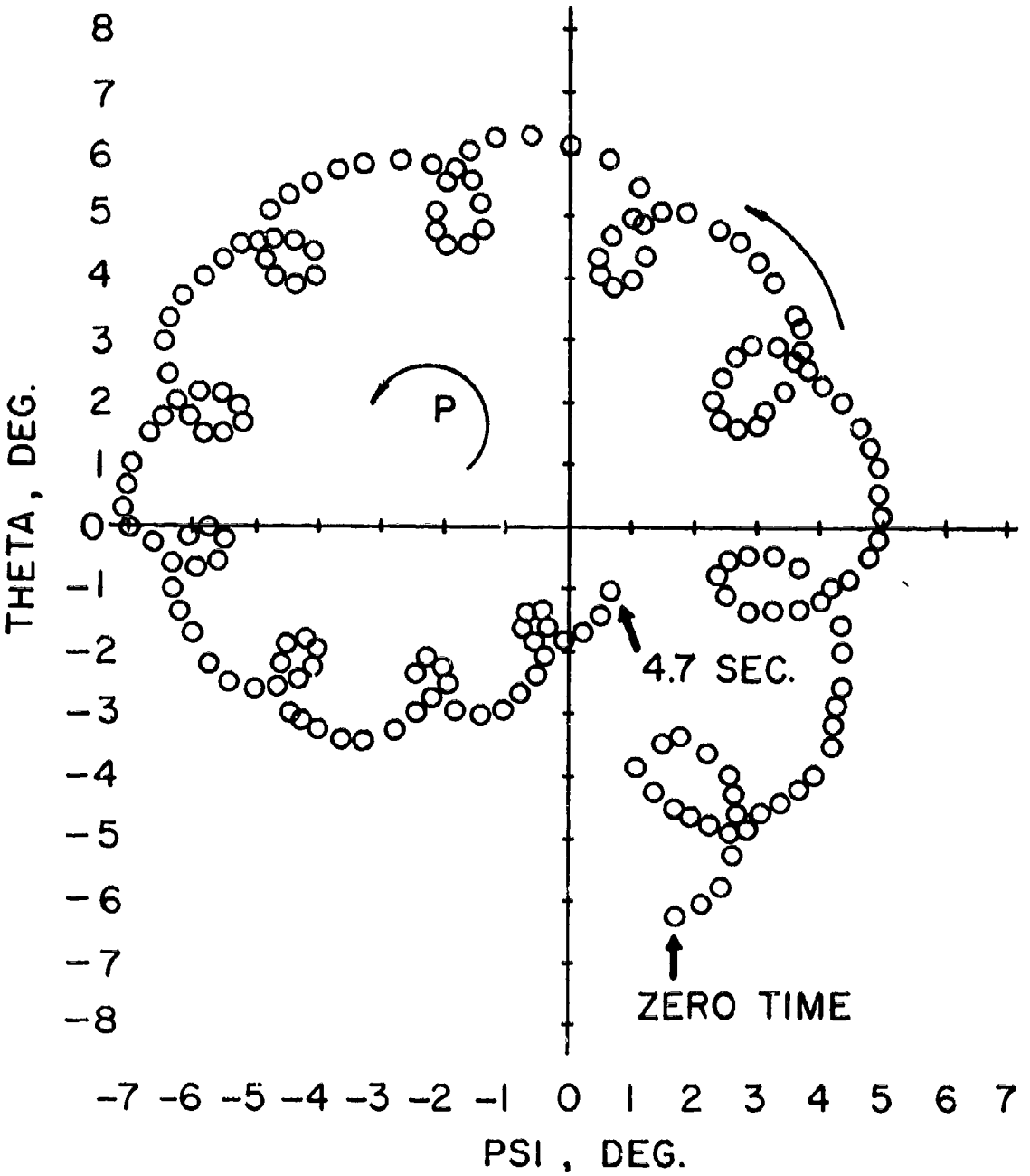

Fig 11 Typical plot of complex angular motion of body with boattail fins (Run 24C, 0.0 to 4.7 seconds)

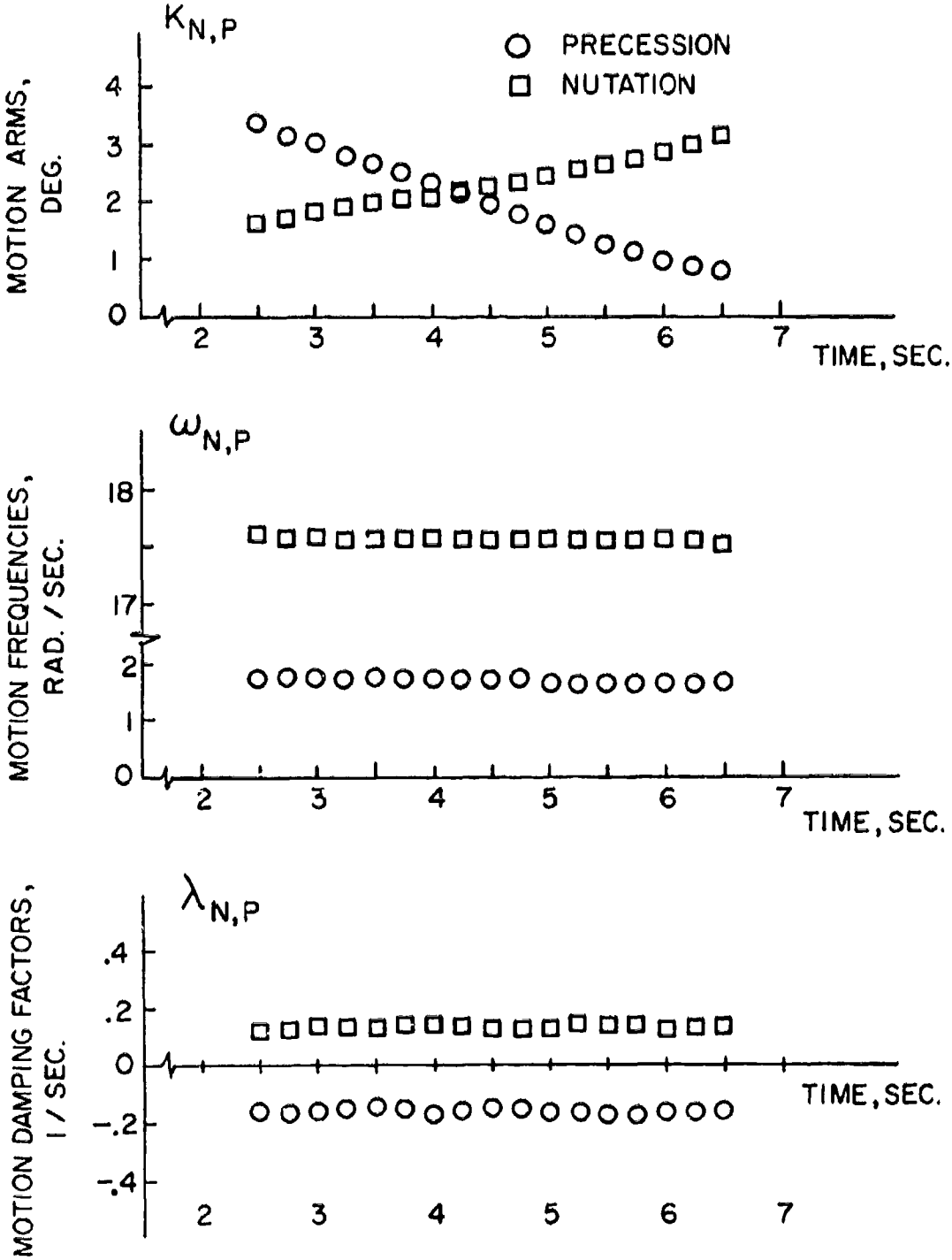

Fig 12 Motion parameters vs time (Run 5C)

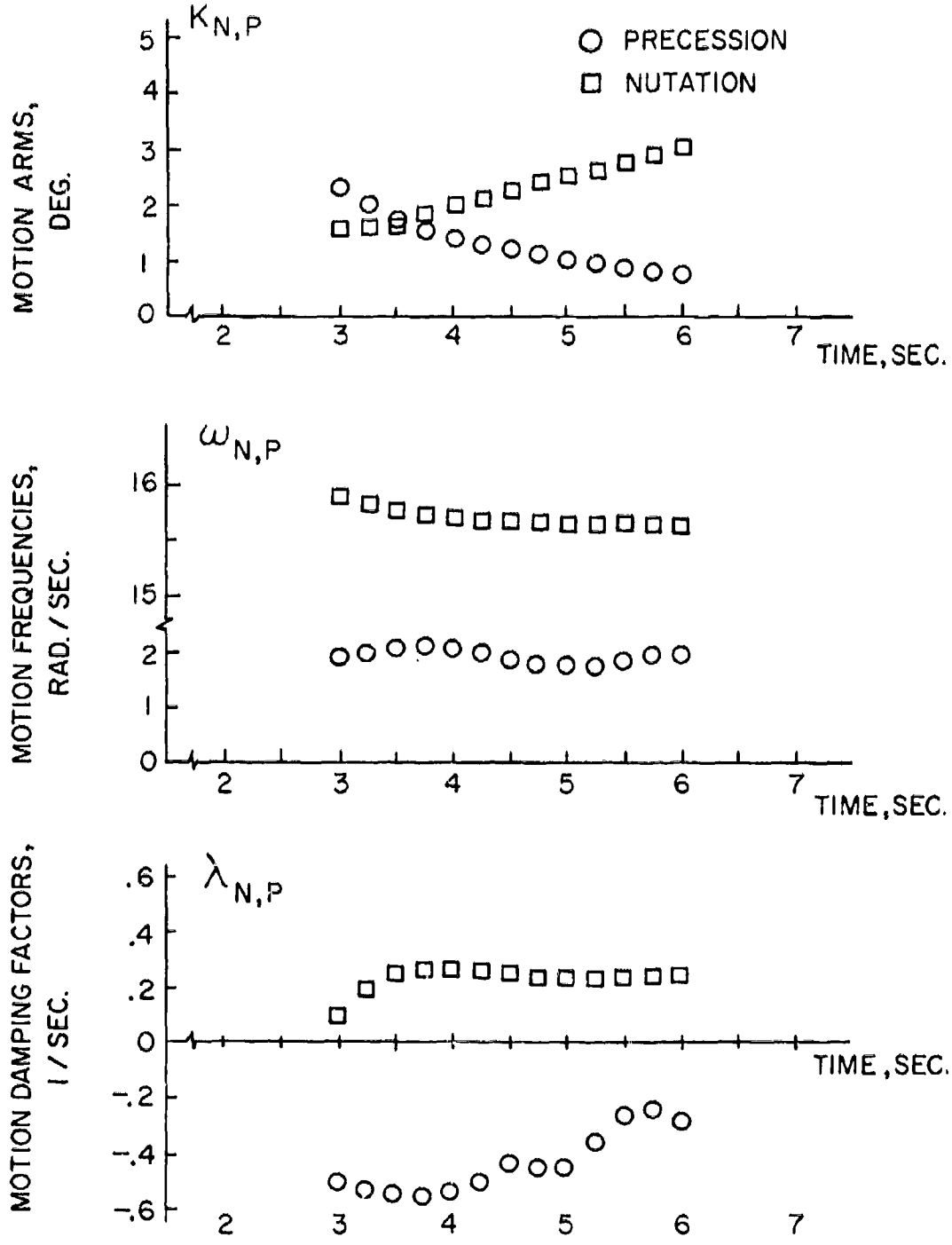

Fig 13 Motion parameters vs time (Run 13A)

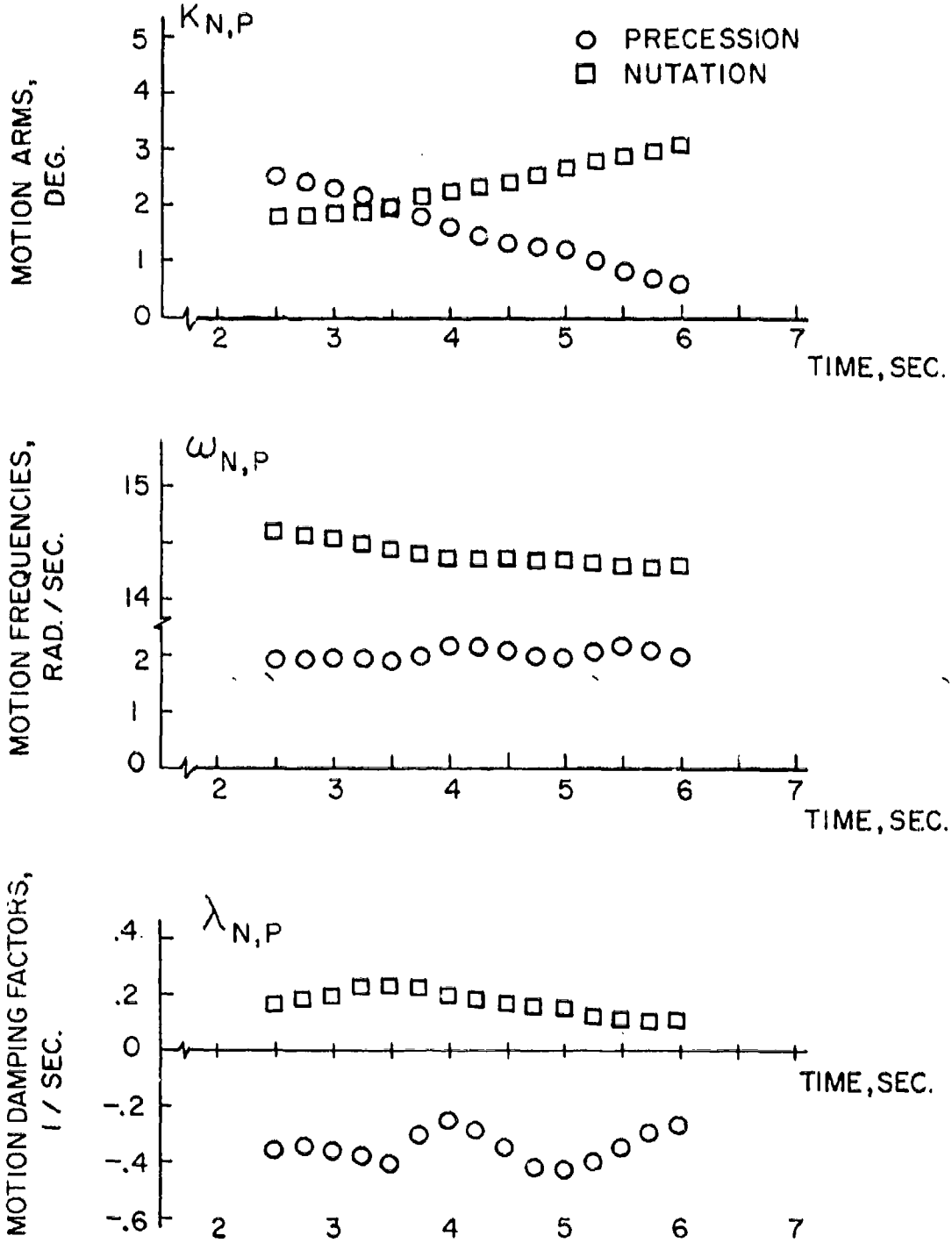

Fig 14 Motion parameters vs time (Run 17A) (body of revolution)

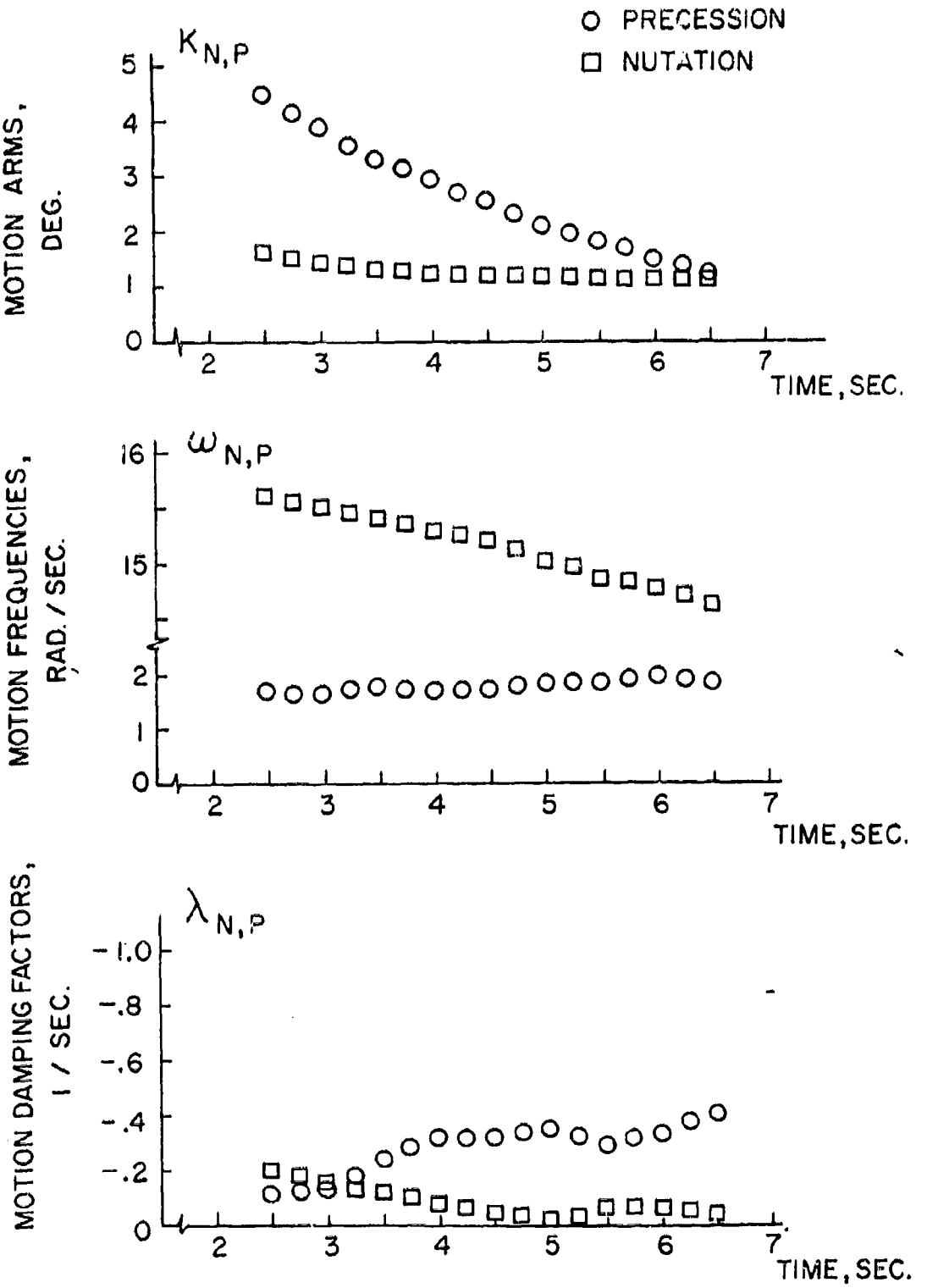

Fig 15 Motion parameters vs time (Run 22B) (with boattail fins)

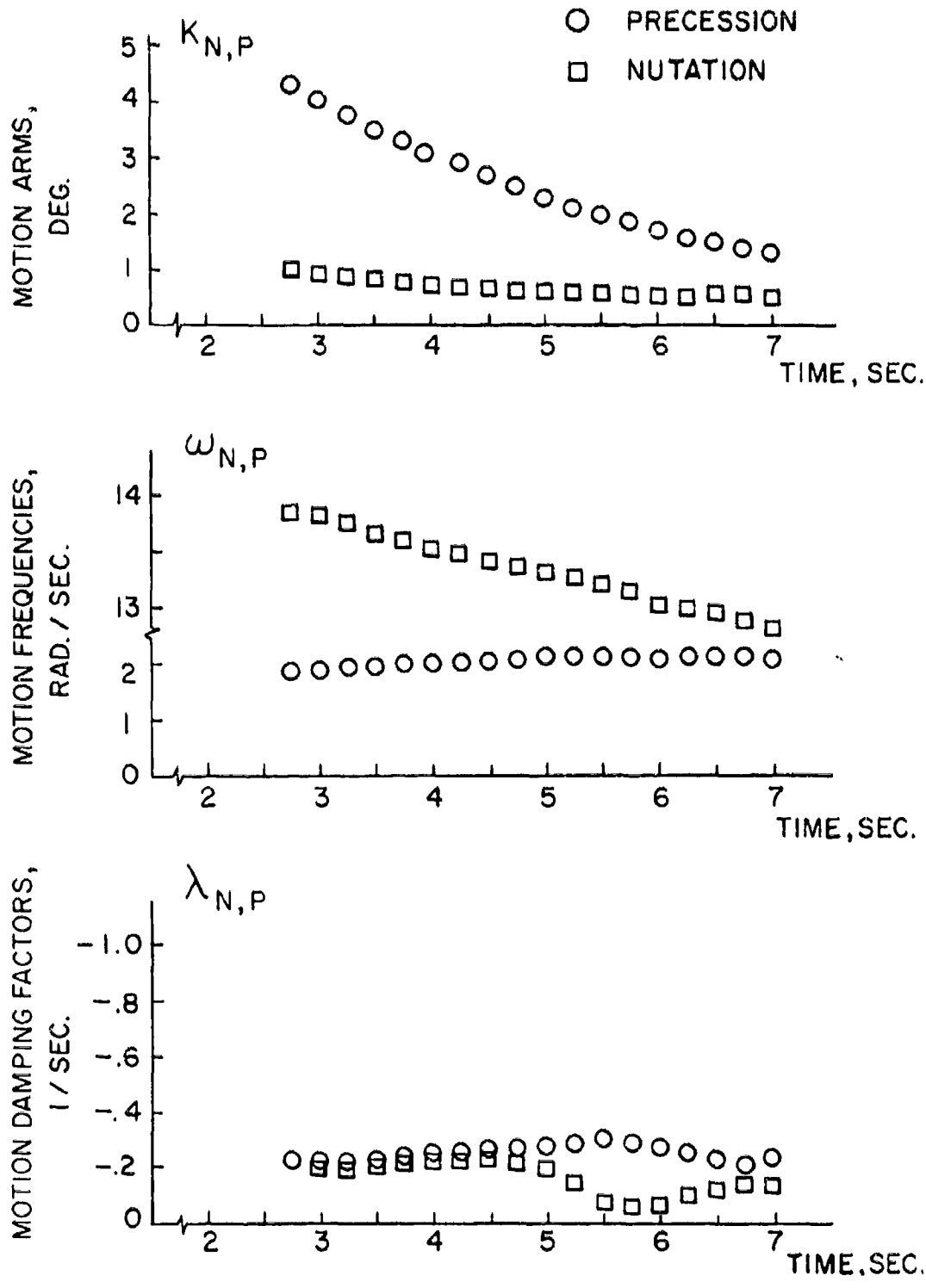

Fig 16 Motion parameters vs time (Run 22C) (with boattail fins)

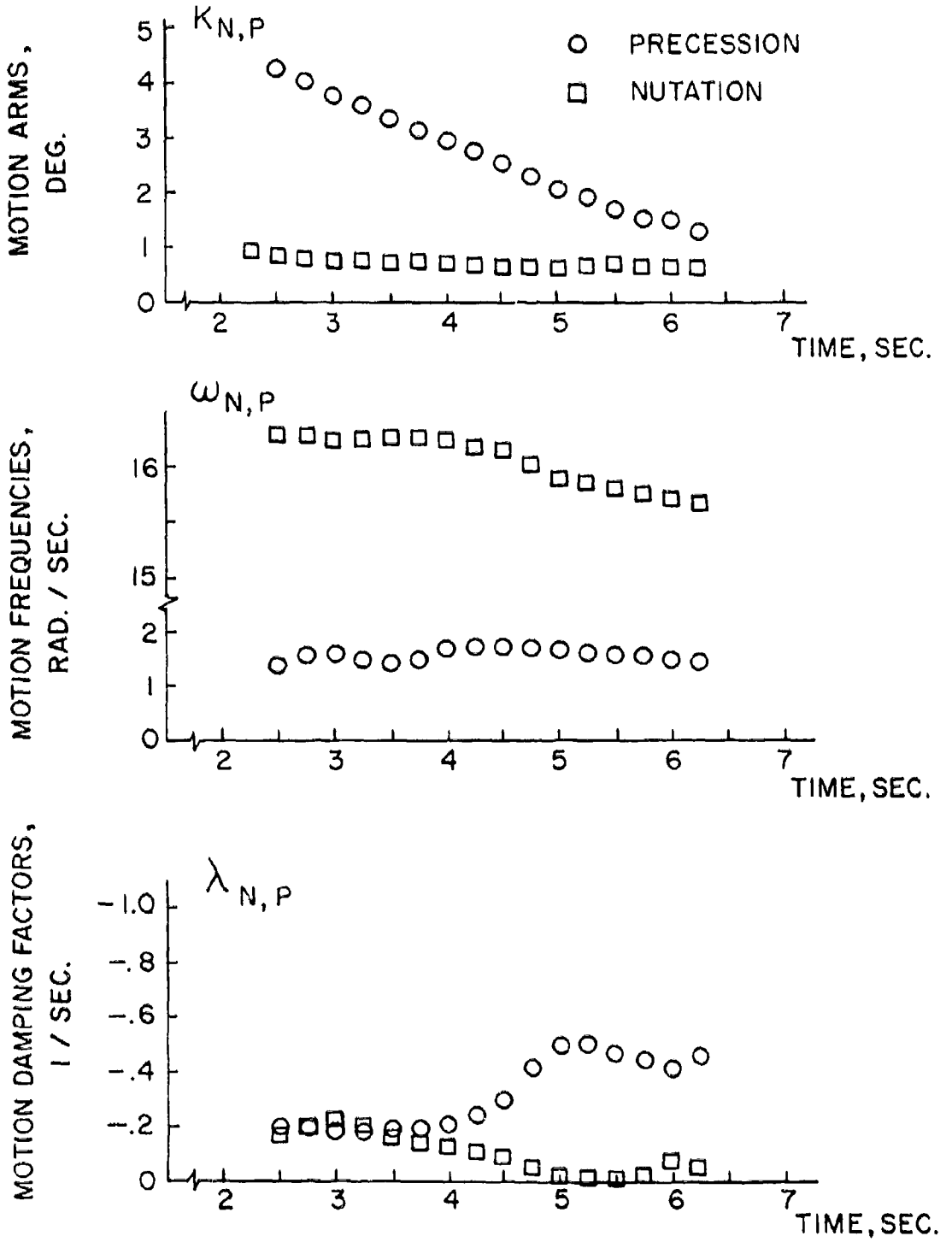

Fig 17 Motion parameters vs time (Run 24C) (with boattail fins)

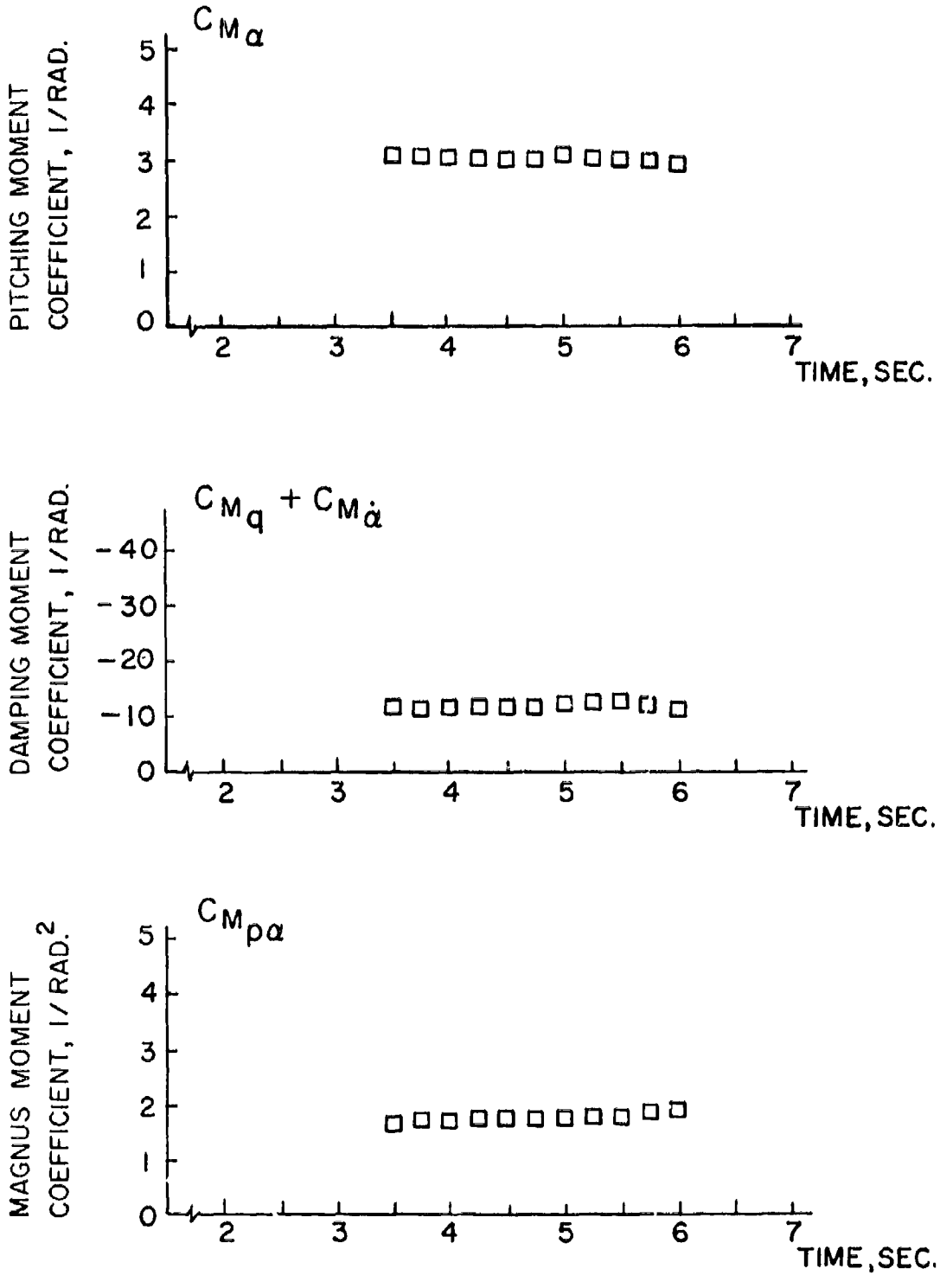

Fig 18 Aerodynamic coefficients vs time (Run 5C) (body of revolution)

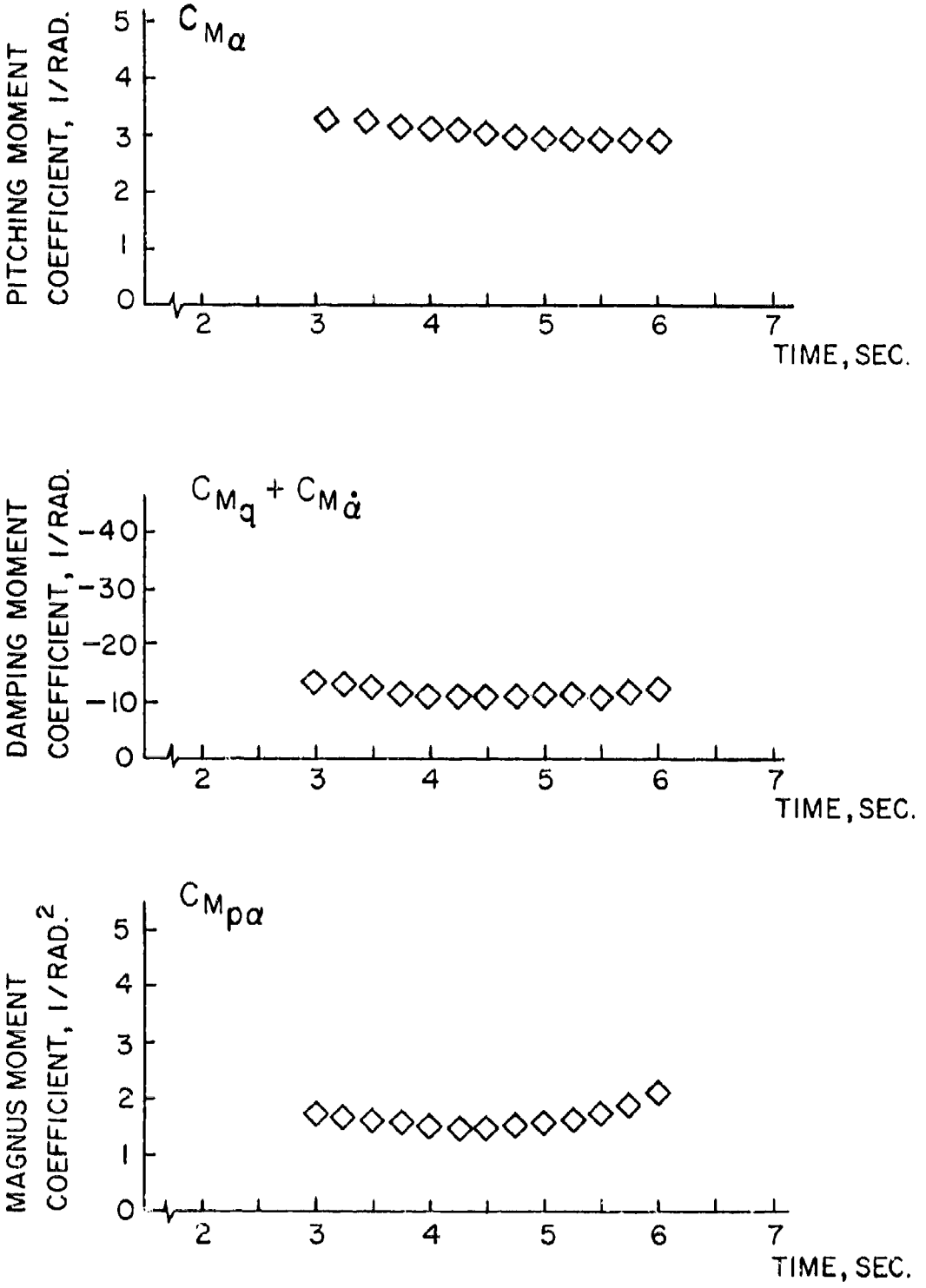

Fig 19 Aerodynamic coefficients vs time (Run 13A) (body of revolution)

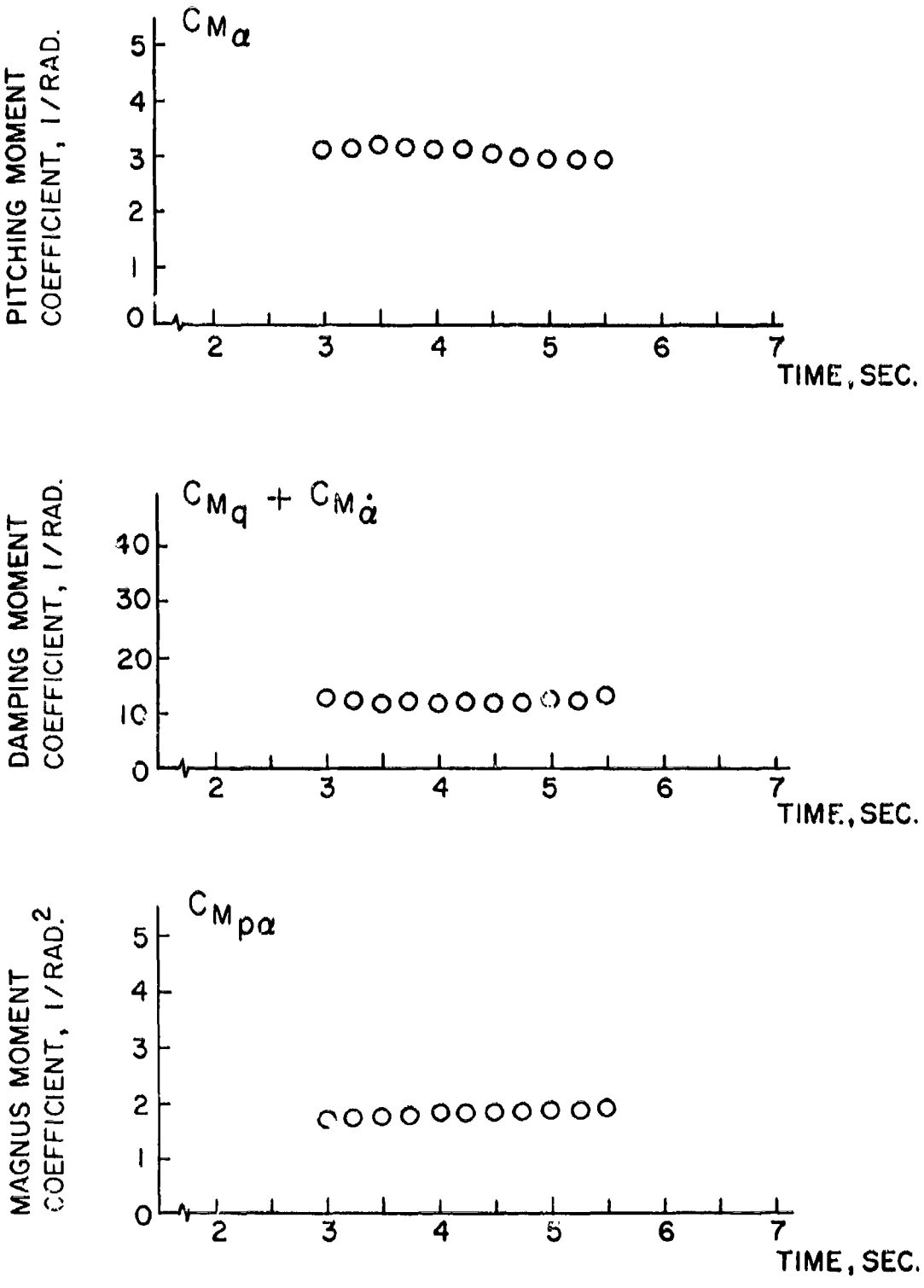

Fig 20 Aerodynamic coefficients vs time (Run 17A) (body of revolution)

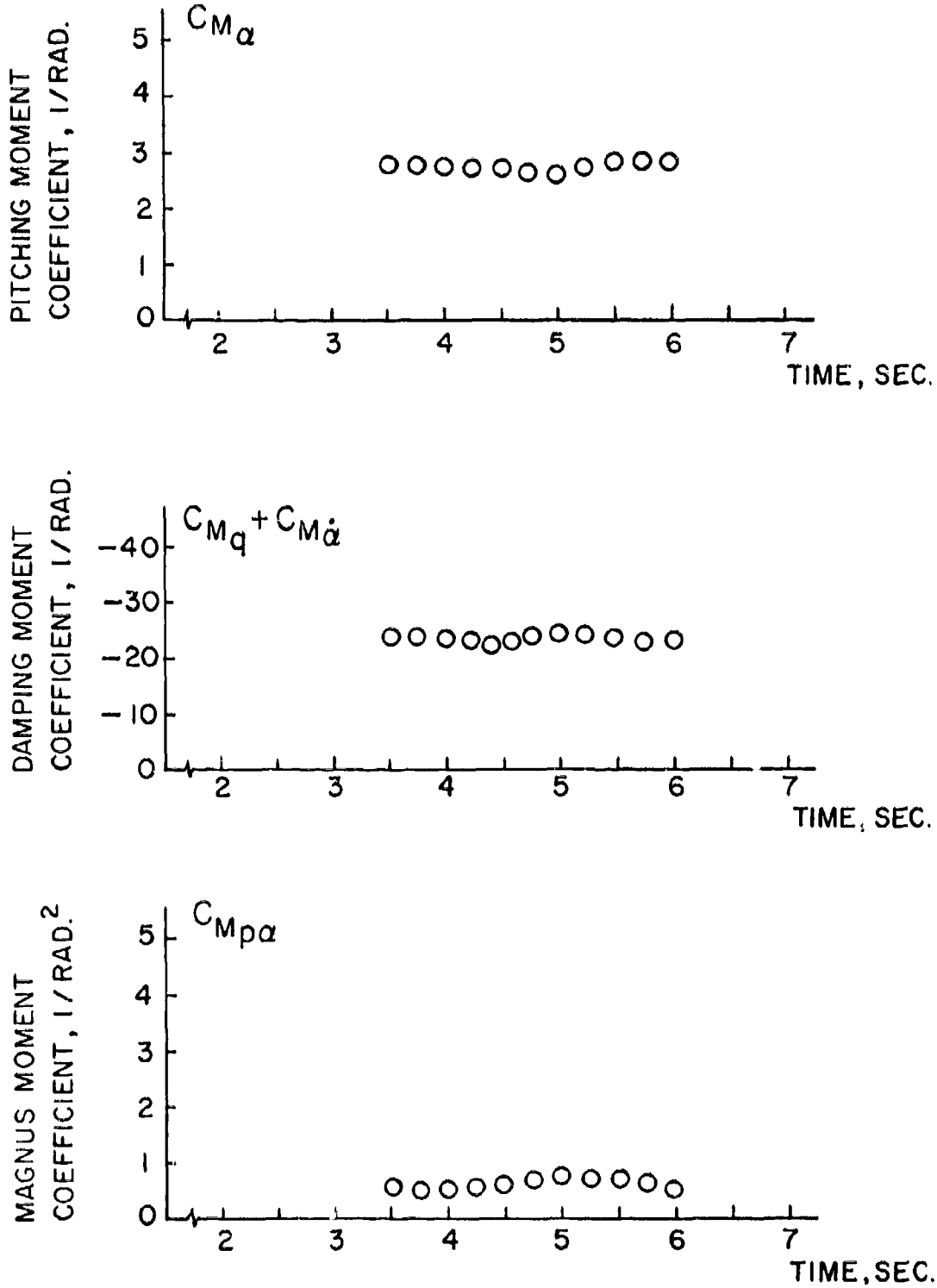

Fig 21 Aerodynamic coefficients vs time (Run 22B) (with boattail fins)

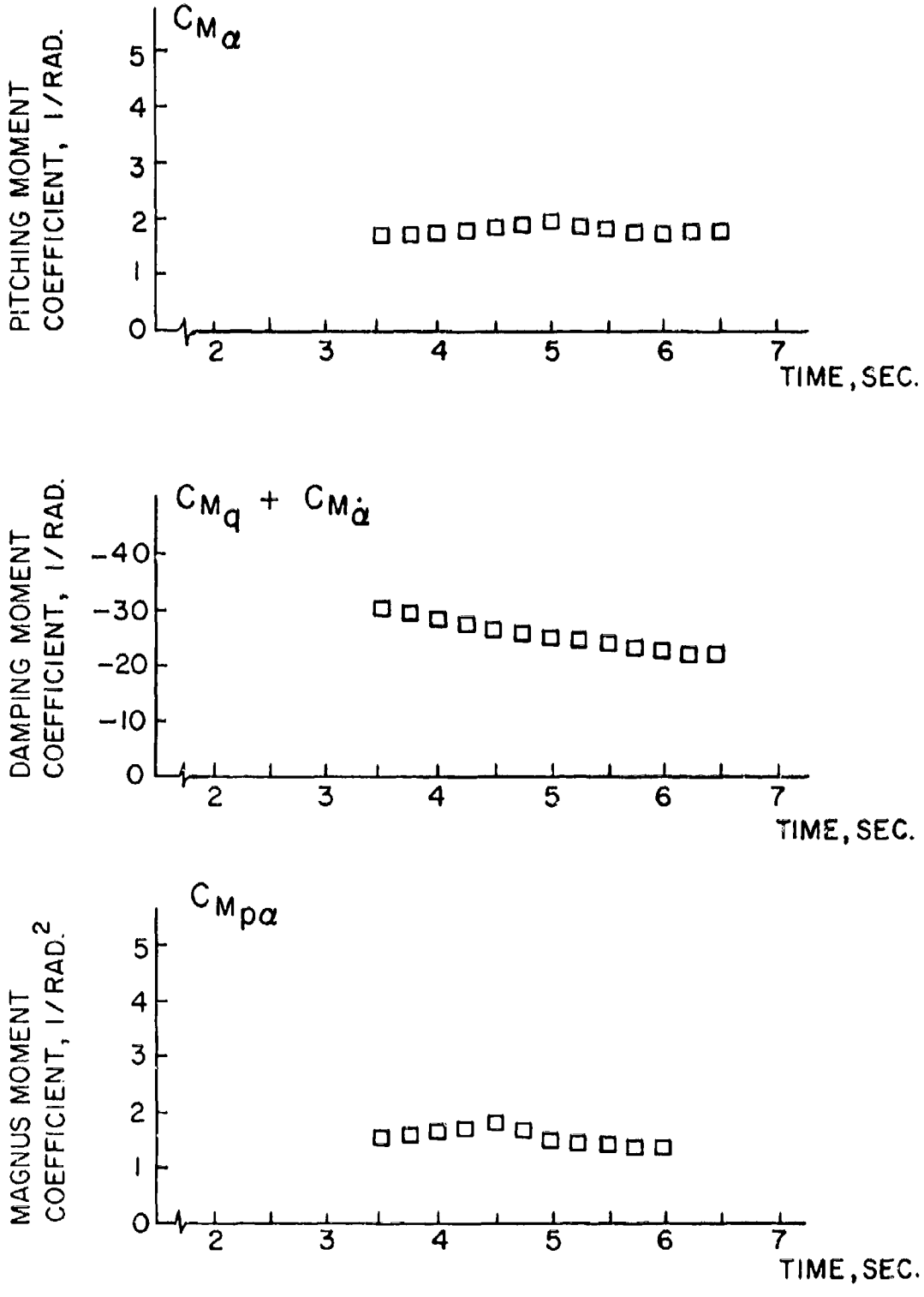

Fig 22 Aerodynamic coefficients vs time (Run 22C) (with boattail fins)

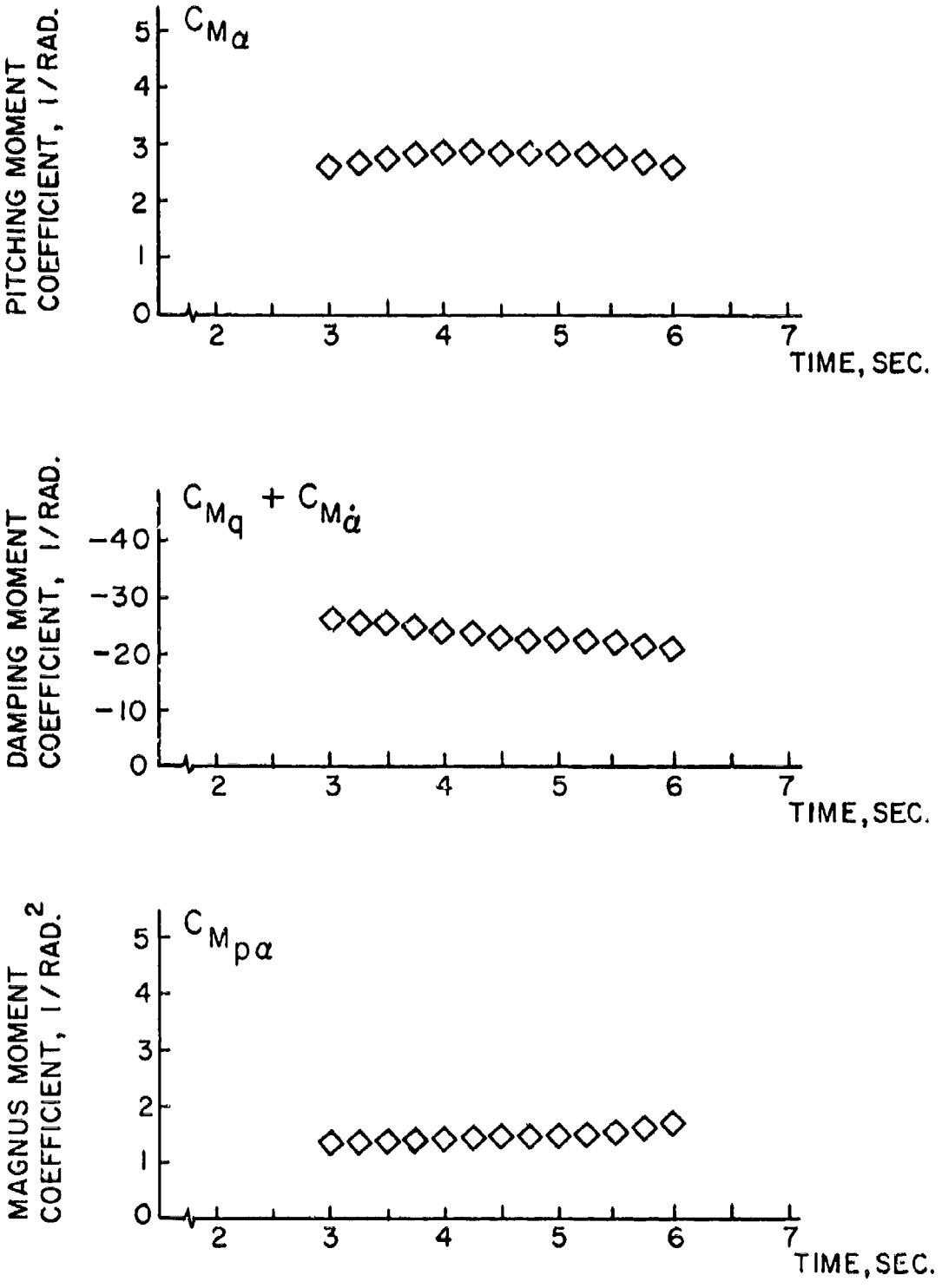

Fig 23 Aerodynamic coefficients vs time (Run 24C) (with boattail fins)

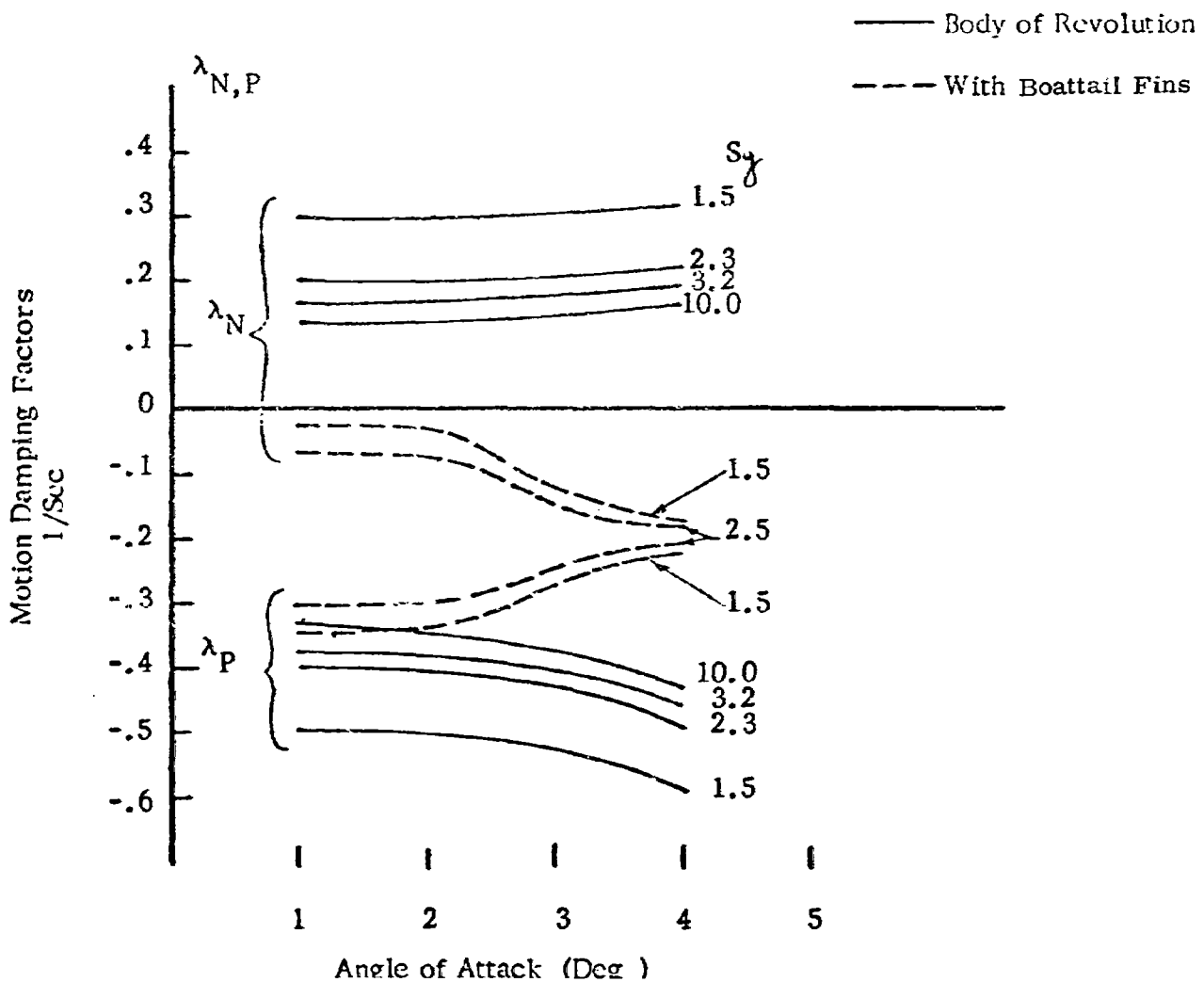

Fig 24 Comparison of damping factors of body of revolution and body with boattail fins at various gyroscopic stability factors (sg)

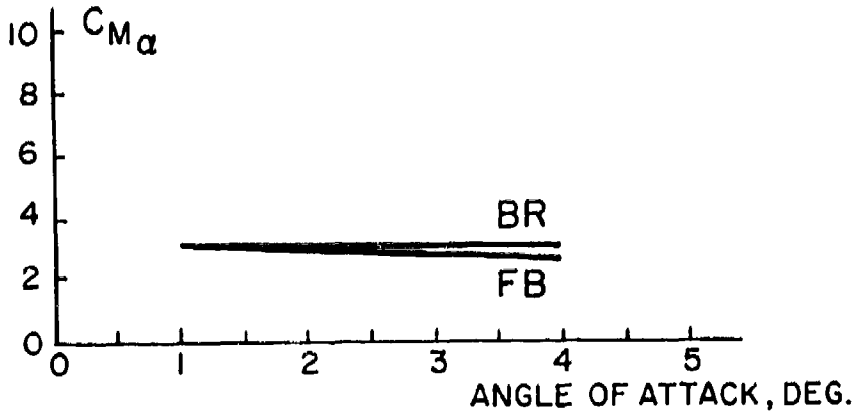

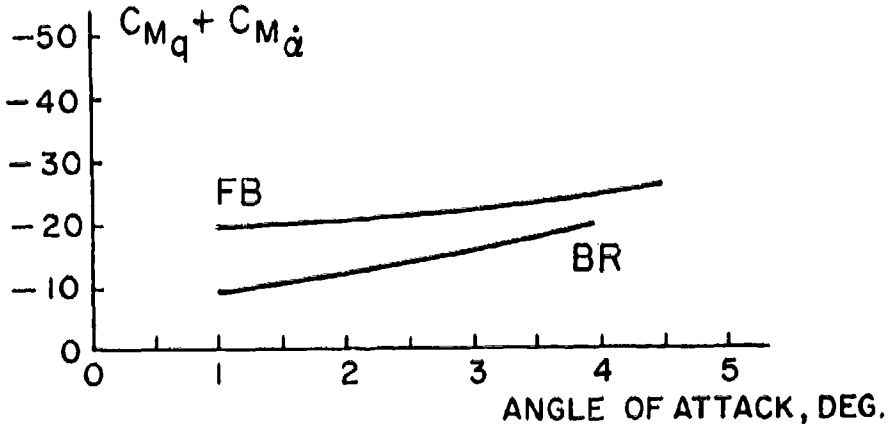

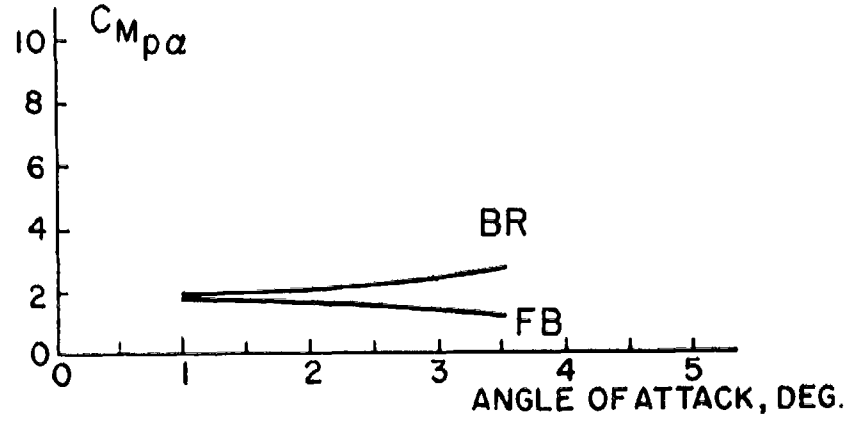

Fig 25 Comparison of the nonlinear aerodynamic coefficients of body of revolution (BR) and body with boattail fins (FB)

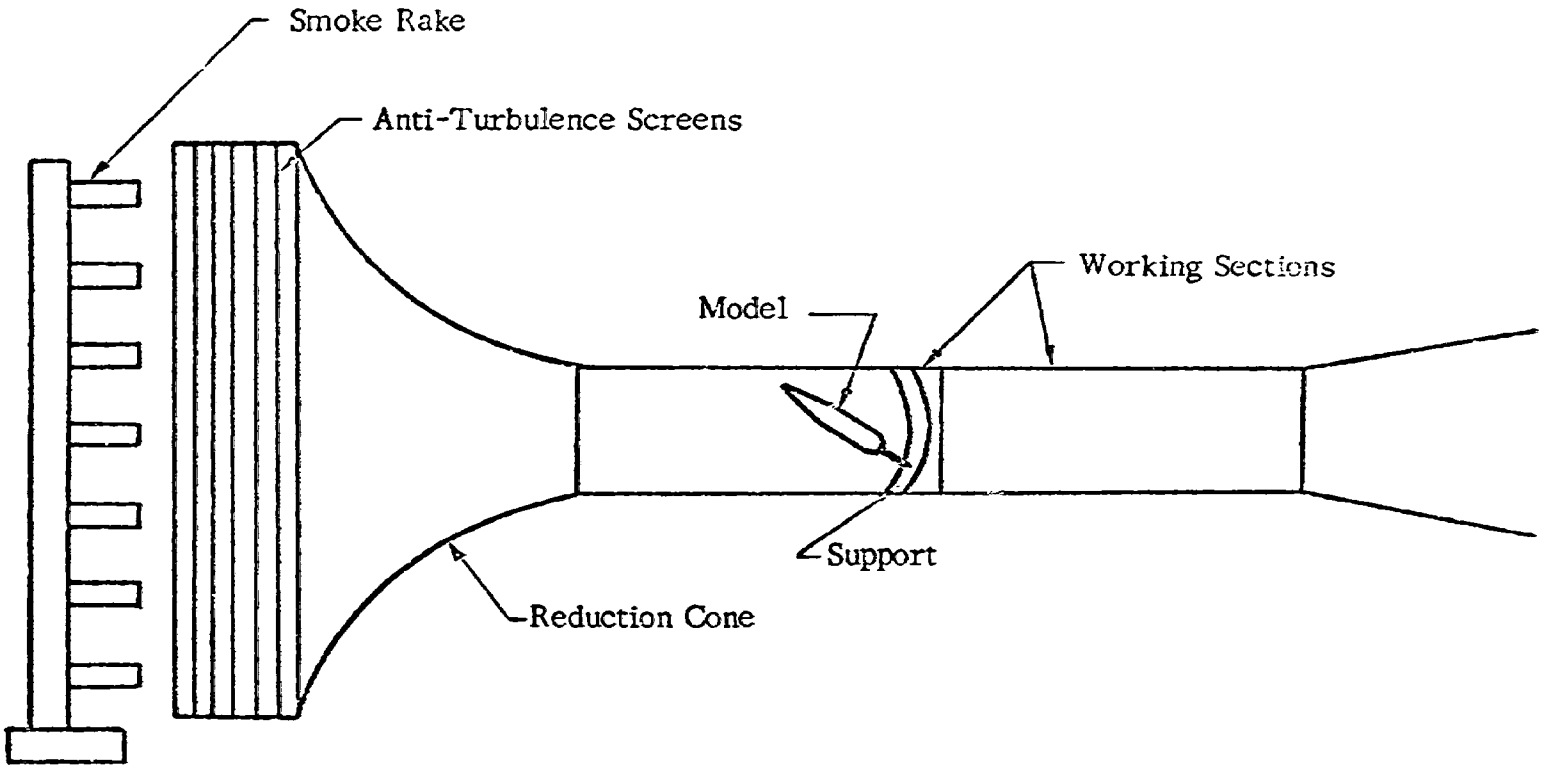

Fig 26 Schematic of smoke tunnel test setup

Fig 27 Smokeflow over the body of revolution at $\alpha = 6^\circ$

Fig 28 Smokeflow over the body with boattail fins $\gamma = 6^{\circ}$

APPENDIX

Theoretical Estimation of Boattail Fin Effectiveness

Modified slender body theory (Ref 7, 15, 17) yields estimated values of the normal force and the pitching moment of the body of revolution of

$$C_{Z_\alpha} \cong -1.5/\text{rad}$$

$$C_{M_\alpha} \cong 3.35/\text{rad}$$

The normal force contribution of the boattail fins may be found using an equation obtained from lifting line theory (Ref 4):

$$C_{Z_\alpha} \cong -\frac{2\pi}{1 + \frac{2}{\text{Aspect Ratio}}}$$

Based on the body cross-sectional area and taking the Aspect Ratio as one,

$$C^f_{Z_\alpha} \cong -.33/\text{rad}$$

This yields a contribution to the pitching moment of -.50, giving,

$$C_{M_\alpha} \cong 2.85/\text{rad}$$

for the finned configuration.

Using Sacks' formula (Ref 5),

$$C_{M_q} \cong \frac{\ell - x_1}{d} \; C_{Z_\alpha} \text{ /rad}$$

the pitch damping moment of the body of revolution was found to be

$$C_{M_q} + C_{M_{\dot{\alpha}}} = -14.2/\text{rad}$$

and for the finned body

$$C_{M_q} + C_{M_{\dot{\alpha}}} = -17.3/\text{rad}$$

The contribution of the boattail fins to the Magnus moment can be estimated by considering the yawing moment produced by the relative difference in incidence of the boattail fin on the right and left side of the body when it is at an angle of attack in the vertical plane. This treatment follows that given for airplanes by Perkins and Hage (Ref 18). The angle of incidence of the descending boattail fin is increased by

$$\delta = \arctan \frac{py'}{V} \qquad (V >> py')$$

and decreased by the same amount on the ascending fin. Resolving the incremental components of lift and drag perpendicular and parallel to the direction of motion and summing the resulting moments about the body by Strip Theory (Ref 1) yields,

$$C_{M_{p\alpha}} = -\frac{C_{L_\alpha}}{3} \; \frac{b}{d}$$

This result is an order-of-magnitude approximation since it does not account for the boundary layer thickness, fin-to-fin or fin-body interference and rectangular fins. This estimated Magnus moment contribution of the boattail fins was found to reduce the average measured value of $C_{M_{p\alpha}}$ of 1.90 to 1.79.

Because of the simultaneous increase of the damping moment and the decrease in the Magnus moment combined with increased gyroscopic stability, the possibility of stabilization of the divergent nutation mode of the body of revolution was indicated.